THESIS

PUBLIC ARCHAEOLOGY AND GEOPHYSICS: SEARCHING FOR UNMARKED HUMAN BURIALS IN RURAL COLORADO

Submitted by

Donald J. Rowe

Department of Anthropology and Geography

In partial fulfillment of the requirements

For the Degree of Master of Arts

Colorado State University

Fort Collins, Colorado

Spring 2023

Master's Committee:

Advisor: Edward Henry

Dennis Harry
Jason LaBelle

ABSTRACT

PUBLIC ARCHAEOLOGY AND GEOPHYSICS: SEARCHING FOR UNMARKED HUMAN BURIALS IN RURAL COLORADO

Rural communities in Colorado are often left in control of lands that potentially contain unmarked burials. Two such communities in Colorado, Gould and Wray, are interested in examining the possible existence of unmarked burials on public lands. The land near the Gould Community Center was used to house prisoners of war during the final year of World War 2 and the community believes mostly fallen concrete markers (one still stands) found at the site may be related to burials from that time. Wray, CO in Yuma County is home of the East Yuma County Cemetery Board (EYCCB), which manages the Kingston and Evangelical Lutheran Cemeteries. The EYCCB took over management of these properties after periods of abandonment and the burial records are lost, this has the left them with potential unmarked burials at each of these sites. The expense and ethical concerns related to accidental disinterment provide rural communities an incentive to locate any unmarked burials on land they manage. I combined four geophysical methods with historical information provided by community partners to determine what areas at the respective sites were most likely to contain unmarked burials. The four methods I employed include: ground-penetrating radar (GPR), electrical resistivity tomography (ERT), electromagnetic induction (EMI), and magnetometry. Using these methods, I was able to locate numerous geophysical anomalies and geolocate them in the mapping software of ArcGIS Pro. In Gould I was unable to determine the source of the geophysical anomalies found due to the wide variety of uses the site has had in the past as well as the lack of historical evidence for burials. Historical evidence of previous burials at the Kingston and Evangelical Lutheran Cemeteries allowed me to make the argument that these anomalies were potentially related to burials. At

Evangelical Lutheran Cemetery I concluded the cemetery is likely to contain unmarked burials throughout the southern half of the site. However, the lack of geophysical markers suggests that the soil in the northern quarter of the site is largely undisturbed and likely does not have burials. I concluded that Kingston Cemetery is expected to contain burials in the south and west of the site. Additionally, the part of Kingston Cemetery that is least likely to contain unmarked burials is the northeastern corner of the site, with a strip along the northern boundary that possibly contains burials.

ACKNOWLEDGEMENTS

I would like to express my gratitude to the communities of Gould and Yuma County Colorado who initiated this project and helped in the collection of the data used in this thesis. A very special thank you to Jean Krause, the local historian in Gould, and to Harry Ivarie, the president of the East Yuma County Cemetery Board. Their support and assistance were essential to the success of this thesis. A special thank you to my advisor, Dr. Edward Henry, whose guidance, support, and encouragement was vital to the completion of this thesis. Additionally, I would like to think the members of my committee, Dr. Dennis Harry and Dr. Jason LaBelle for their assistance in the completion of my thesis. Thank you to my close friend, Micah Mayle, who helped me with data collection and interpretation as well as editing of this thesis. Finally, I would like to thank all my family and friends whose support and encouragement allowed me to complete this thesis.

TABLE OF CONTENTS

Chapter 1: Introduction

Burials are a way for people to memorialize their dead (often with markers) and are typically placed at sites of sentimental and religious importance. Sites containing burials are linked to living communities, which may be abandoned as time progresses. When small communities are abandoned, the dead are left behind. If these sites are not maintained then over time information about these burials, specifically the physical records, are lost (i.e., markers degrade, are destroyed, or are buried). Spread across rural Colorado one can find many abandoned cemeteries that have seen their associate communities disappear. These sites often eventually pass into the care of nearby rural communities, many of which are home to descendants of the interred. For these communities the risks of unintentionally disinterring unmarked burials creates ethical and financial challenges. This makes the use of surrounding land difficult for these rural communities. Therefore, knowing potential locations of unmarked burials is beneficial for those interested in local histories and those hoping to excavate areas where they may be present (Conyers, 2006; Laderman, 2003; Lemke, 2020; Rugg, 2000; Sanger et al., 2020).

I investigated potential unmarked burials at three separate locations in Colorado. They include a community center in Gould, Colorado as well as Evangelical Lutheran and Kingston Cemeteries in Wray, Colorado (Figure 1). In each case, local community members reached out to the Center for Research in Archaeogeophysics and Geoarchaeology (CRAG) at Colorado State University for help investigating these locations and their internal organization. Community members at these three sites are interested, for both historical and practical reasons, in learning about the potential for unmarked burials. For instance, there is interest in gaining a better understanding of the local histories of these locations by identifying possible unmarked burials that represent examples of place making associated with the small communities with which they were originally associated (Miller & Rivera, 2006; Rugg, 2000; Sudradjat, 2012; Vidler et al., 2014). Identifying extant burials is considered both a way to connect sites to people that once lived nearby and a way for community members living near those sites today to build a sense of place more strongly as it relates to these sites. The separation of the dead from the living helps define what space a community should occupy, and the definition of their space is only strengthened by knowledge of the places that have been left for the dead (Miller & Rivera, 2006; Rugg, 2000; Sudradjat, 2012; Vidler et al., 2014). Additionally, the public ownership of cemeteries forges a sense of community between families that can last for multiple generations. Practical concern in identifying extant burials is related to the prevention of their disturbance and the furthering of their preservation. Kingston Cemetery is currently the only site under consideration by the East Yuma County Cemetery Board (EYCCB) for resumed use. However, delineation of areas that are likely to contain burials allows for less uncertainty in the management of all three sites.

I divide my discussion of these sites according to their geographic locations and the presence, or absence, of marked burials. Gould Community Center is in the North Park Basin of the Colorado Rockies near the community of Gould, CO (Figure 1). The Gould Community Center has no marked or known burials. However, there are several unmarked concrete markers reminiscent of stele, commonly used as grave markers, visible across the site. The period of possible mortuary activity at the site spans late 1944 through early 1946. Both Kingston Cemetery and Evangelical Lutheran Cemetery are in Yuma County Colorado near the border shared with Nebraska and Kansas (see Figure 1). The closest community to both these far eastern cemeteries is Idalia, CO, however they also have connections to communities like Wray, CO and former communities like Kingston, CO. These sites are further divided by the presence of existing marked burials at the cemetery sites. The two cemetery locations in Yuma County have marked burials dated between the late 19^{th} and early 20th centuries, the latest of which can be found in Kingston Cemetery dated to 1942.

The communities' desires to locate burials without disturbing or disinterring the burials made non-invasive archaeological methods ideal. Efforts to locate unmarked burials using archaeology have often included geophysical applications (Bigman, 2012; Conyers, 2006; Johnson, n.d.; Lemke, 2020; Moffat, 2015; Sanger et al., 2020; Sea & Ernenwein, 2021; Thompson et al., 2018). I carried out a multi-instrument geophysical survey to evaluate the potential for unmarked burials at each site utilizing ground-penetrating radar (GPR), electrical resistivity tomography (ERT), electromagnetic induction (EMI), and magnetometry (Bigman, 2012; Billinger, 2009; Conyers, 2006; Moffat, 2015; Sanger et al., 2020; Sea & Ernenwein, 2021; Stanger & Roe, 2007; Thompson et al., 2018). Using data from these methods, I created several subsurface visualizations of each site. These visualizations helped me to establish what portions of each site contain anomalies that could correlate with potential unmarked burials, as well as what areas appear to be undisturbed. In considering these sites, historical information related to each site and geophysical research done in similar environments will be used to analyze the results of my multi-instrument survey. This geophysical investigation for unmarked burials is the focus of my Master's research with a component including the transfer of my results to the respective communities who manage each site.

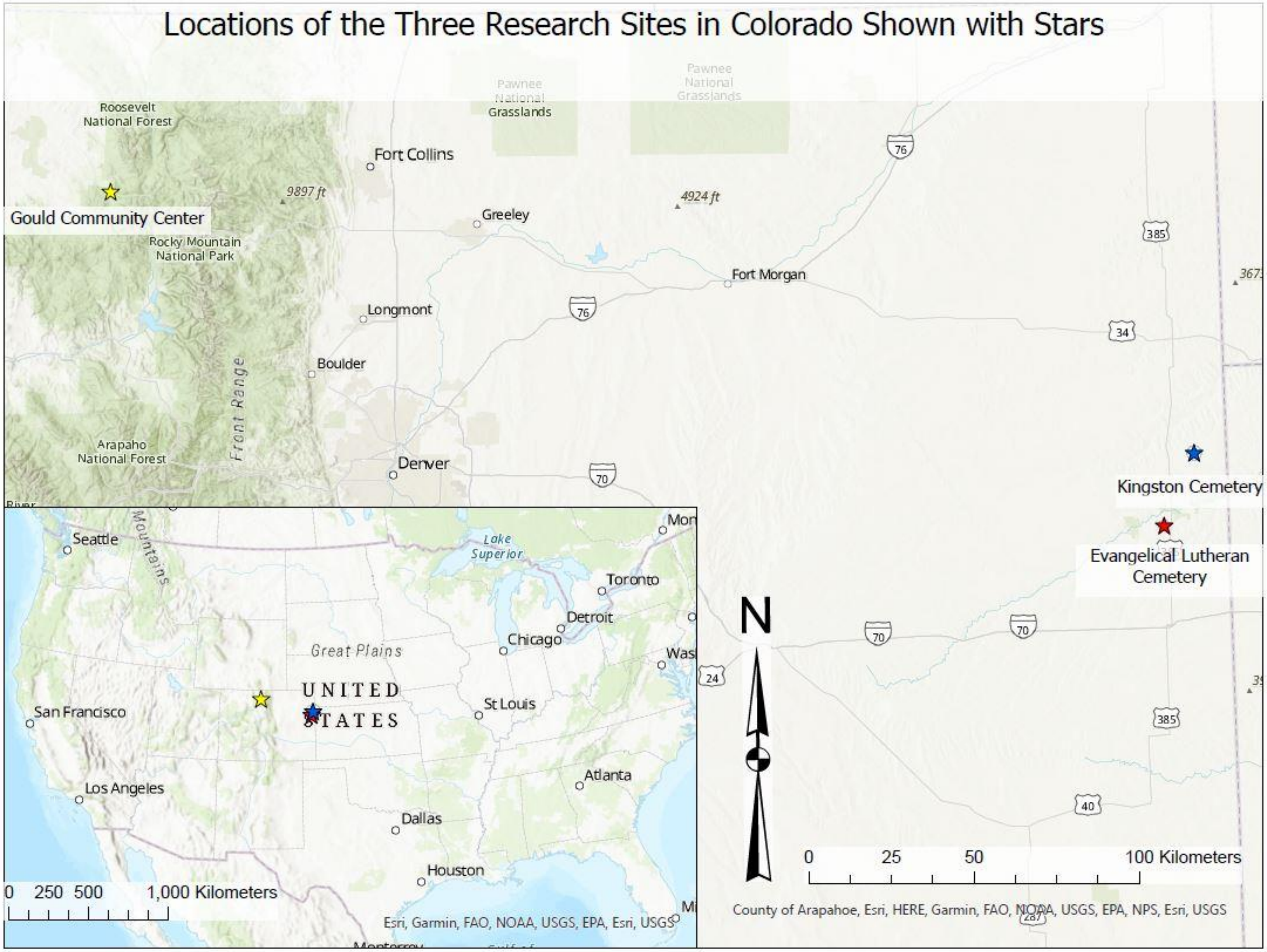

Figure 1: Map of Northeastern Colorado with research sites.

In chapter 2 I review the literature covering the history and geology of the sites I investigated. In providing a historical background of the sites, I contextualize the uses of the land on which the cemeteries are located, as well as the communities who constructed and used these cemeteries. My description of the near surface geology for each site provides context for the results of the geophysical surveys. Finally, the chapter will briefly discuss some successful examples of geophysical methods being employed in cemetery archaeology. Chapter 3 will be an overview of GPR, ERT, EMI, and magnetometry. The chapter will continue with descriptions of the geophysical survey designs and discuss their implementations at the three sites. Data processing and the software used for each method will also be discussed. In chapter 4 the geophysical results will be presented. Chapter 5 will show my interpretation of the results. This will be done by combining the geophysical results and historical information to determine the areas within each site that are most likely to contain unmarked burials. In chapter 6 I will conclude with a summary of my research and discuss the application of combined geophysical techniques in locating unmarked graves for communities. Additionally, potential future steps and possibilities for future research will also be presented.

Chapter 2: Site History, Geology, and Geophysical Techniques in Cemetery Archaeology

Site Histories

The Gould Community Center, Kingston Cemetery, and Evangelical Lutheran Cemetery are all located in rural Colorado, which was first occupied by Native Americans for thousands of years prior to American colonization. The Gould Community Center, located in the North Park Basin of the Colorado Rocky Mountains, resides on land which was taken from the Ute people. Present day Yuma County Colorado where both Kingston and Evangelical Lutheran Cemeteries are located was taken from the Cheyenne and Arapahoe peoples (Abbott et al., 2013a).

The establishment of the state of Colorado began as settlers and prospectors started moving to California and Oregon. With the discovery of gold in the Colorado Rocky Mountains during the 1850's the future state became a destination for settlers moving west looking to make a fortune (Abbott et al., 2013b). During the 1860's the increased settler population lead to increasing bouts of violence between white settlers and Native Americans. Native people were steadily driven from their land as violence, combined with increased outbreaks of disease and famine, forced them into surrender to the United States government. This in turn lead to their internment in government designated reservations. Examples of the violence include the 1864 Sand Creek Massacre and the 1868 Battle of Beecher Island (Abbott et al., 2013a). The violent removal of Native Americans left the rural portions of the state open. Post-Civil War policies of the United States government encouraged the settlement of large tracks of land by settlers from the eastern states (Abbott et al., 2013a).

Kingston and Evangelical Lutheran Cemeteries are both located in modern day Yuma County, Colorado. Modern Yuma County was originally a part of the vast Weld County that until 1887 included the lands of 13 modern northeastern Colorado counties as reported by Abbott et al (2013). In 1887 Washington County was the first modern county carved out of Weld County by the state legislator. Yuma County was formed in 1889 from the eastern half of Washington County which consists of the northern portions of present-day Yuma County. This includes the larger towns along Highway 34 and Wray, CO which became the county seat in 1902 and persists today (Abbott et al., 2013b). The southern part of modern Yuma County was added when the eastern portions of Arapahoe County were partitioned between Washington and Yuma Counties in 1903. This resulted in the current Yuma County with Nebraska and Kansas at its border and an area of approximately 2,379 square miles (Abbott et al., 2013b). Both Kingston and Evangelical Lutheran Cemeteries were established in what was then Arapahoe County but were abandoned by their original authorities after falling into the boundaries of Yuma County. The cemeteries came into the care of the EYCCB in the 1990's, Kingston Cemetery was surveyed by the district in 1990 to document surviving markers and Evangelical Lutheran Cemetery was rededicated as a cemetery in 1999 when the land was turned over to the county.

Kingston Cemetery, also known as the Lansing Valley Cemetery, is located about eight miles northeast of Idalia, CO and approximately seven miles south of the recorded site for the 1868 Battle of Beecher Island (Abbott et al., 2013a). The cemetery was originally associated with the small rural town of Kingston, CO. The town's name was changed to Lansing as early as 1887 as pointed out by Homm (1997). Evidence of the new town name can be seen in the 1893 article of The Denver Press, "A Postmaster Murdered" covering the killing of the town's postmaster. Lansing was one of many small rural communities that were formed in the 1880's after a period of heightened rainfall had made this area of the plains ideal for agriculture (Abbott et al., 2013b). However, drought conditions began in the early 1890's and peaked in 1894 when only ten inches of rain were recorded in the nearby town of Yuma, CO. Thus, agriculture struggled and by the 1890's the town and much of eastern Colorado began to see a decline in population. The total population of the eastern counties dropped by as much as 40 percent throughout the 1890's leading to the abandonment of several small communities (Abbott et al., 2013b). Lansing continued to be referenced in maps of Colorado as late as 1911, but by the 1920's the name disappears as the remaining residents relocated to nearby towns (Homm, 1999). The cemetery was used periodically after the town was dissolved as the last marked burial dates to 1942. Relatives of those buried here still live in the surrounding area, either on rural farms or in nearby towns like Idalia or Wray.

Evangelical Lutheran Cemetery began as a graveyard for the Evangelical Lutheran Salem Church and is located approximately nine miles south of Idalia, CO. The wood and sod church as well as the associated cemetery were built in 1888 on land donated by individuals identified as Mr. Luessenhop and August Handke, respectively (Homm, 1999). Evangelical Lutheran Cemetery served families living between the south fork of the Republican River and Landsman Creek. There are references to a community known as Landsman on a map of the area created in 1886 and in a newspaper known as *The Brush Lariat* dated 1885 (Gray, 1886; "Haigler," 1885). Like Lansing, the families in Landsman began to migrate away from the area in the 1890's. The church and graveyard fell out of use in the early 1900's, with the last marked burial being dated at 1908. The church structure was disassembled in the early 1900's by two men, Nanne Boden and Bill Zick, who divided up the lumber from the structure (Homm, 1999).

The Gould Community Center lies around two miles southeast from the community of Gould, CO and approximately twenty miles southeast of Walden, CO. Before serving as the location of a community center the land was initially utilized for timber harvesting. The site had various occupants including a Civilian Conservation Corps camp from 1935-1944 as well as, a prisoner of war camp from 1944-1945. Between 1946-1986 the land hosted a 4-H Club and as of 1986 has served as the community center for the town of Gould (Worrall, 1990). The local community expressed interested in potential unmarked burials related to the lands use as a prisoner of war camp. The prisoners that were put to work at this location were German prisoners from the second World War (Bradley, 2005). This camp near Gould was associated with the larger camp in Greeley, CO known as Camp 202 which operated from 1943 until 1946 (Worrall, 1990). The Michigan River Timber Company contracted prisoner labor from the Greeley camp for timber harvesting between May of 1944 and October of 1945 (War Department vs. Michigan River Timber Company, 1944). During this time, there were 300 men split between several timber camps, including the site in Gould. The Michigan River Timber Company agreed to pay the United States government $67,500 for 90 prisoners to work for 150 days. In this agreement the contractor agreed to work the prisoners a maximum of six, eight-hour days per a week, “falling, peeling, and cutting telephone poles” (U.S. Department of Veterans Affairs, 2023). Additionally, the contract indicates that the prisoners would be kept at State 4-H Club Camp 3, located approximately three miles east of Gould and that they were forbidden from being used for the most dangerous types of work (War Department vs. Michigan River Timber Company, 1944). The local community believes there may be German prisoners that were buried at the camp specifically above the floodplain of the Michigan River that borders the community center in the south. This area has multiple toppled and partially buried concrete markers that resemble grave markers, as well as one marker that is standing in a small clearing. There are German prisoners buried at Veterans Affairs National Cemeteries throughout the United States, including one known burial in a Denver cemetery that dates from World Wars II (U.S.

Department of Veterans Affairs, 2023). However, local historian and community partner, Jean Krause, found no evidence of burials, or any description of deaths associated with the site in Gould.

Geology and Physical Landscape

Colorado straddles the boundary between the Rocky Mountains and the Great Plains of the American West. Western Colorado is dominated by the Rocky Mountains, Great Basin, and desert environments of the Four Corners Region of the United States and hosts the site in Gould, CO. Eastern Colorado consists of the Great Plains of the central United States and hosts the Kingston and Evangelical Lutheran Cemeteries.

Gould, CO is located approximately twenty miles southeast of Walden, CO in Jackson County and falls in the mountain west of the state. The site is in North Park, a basin in the Rocky Mountains of northern Colorado, at an elevation around 2,700 meters. The site is along the northern side of the Michigan River, a headwater of the North Platte River, which flows through a glacial valley carved during the Pleistocene (Madole, 1991). The underlying geology reflects the glacial history of the valley with deposits from the Pleistocene cut by Holocene alluvium deposited by the Michigan River. The source material for the glacial till and alluvium are the igneous rocks dating to the Miocene and Oligocene (Madole, 1991). Soils that have been documented overlying such geology are rich in clay and include a mix of clast sizes ranging from clay size particles up to large boulders. This clast mixture is often associated with glaciers. The climate of the area is semi-arid with large amounts of frozen precipitation during the winter which promotes a landscape that is covered in coniferous forest. This has historically attracted timber harvesters to the area resulting in regular removal of the forest and regrowth. This results in dense coverage by small conifers and large amounts of ground clutter throughout the site. The portion of the land occupied by the Gould Community Center that is thought to possibly contain burials is located along the edge of the small flood plain of the Michigan River (Figure 2).

Figure 2: Survey area corresponds to the extent of the concrete markers near the Gould Community Center, the location of the standing marker is indicated.

In eastern Colorado the climate is semi-arid, with low humidity and infrequent precipitation that is concentrated between April and September. The native vegetation is dominated by short grasses that are common to the western portions of the Great Plains. The geologic setting of this area is dominated by thick silty soil deposits of the Peoria Loess which resulted from Pleistocene glaciation and subsequent eolian deposition (Muhs et al., 2008). The Kingston and Evangelical Lutheran cemeteries have no recorded disturbance outside of the burials since they were established in the 1880's. However, these sites are ideal for burrowing animals like prairie dogs and ground hogs, as evidenced by numerous animal burrows across both sites. Evangelical Lutheran Cemetery is approximately three-and-a-half miles southwest of the confluence of the South Fork of the Republic River and Landsman Creek. The cemetery is approximately 20 by 70 meters in size and is bounded by barbed wire fence to the south and east while a line of trees forms the western and northern boundary (Figure 3). Kingston Cemetery is a square plot of land that is approximately 100 by 100 meters in size and can be found on the East side of County Road LL where it is bounded on all sides by barbed wire fencing (Figure 4). The nearest town to both Kingston and Evangelical Lutheran Cemeteries is Idalia, CO.

Figure 3: Evangelical Lutheran Cemetery with the locations of the known markers and the land historically believed to have hosted the Evangelical Lutheran Salem Church indicated.

Figure 4: Kingston Cemetery with the locations of known markers indicated.

Geophysical Techniques

Ground penetrating radar (GPR) is the most common geophysical technique used in locating unmarked burials (Billinger, 2009; Conyers, 2006; Moffat, 2015; Sanger et al., 2020; Thompson et al., 2018). This is because the method is both effective in this application and is relatively easy to deploy (Conyers, 2006; Moffat, 2015). The method has a proven efficiency in locating burials in a variety of mortuary settings, including both historical and modern cemeteries. Features commonly associated with burials that are revealed using GPR include: buried remains, disturbed soils related to grave shafts, and voids in the subsurface (Burger et al., 2006; Conyers, 2006; Goodman & Piro, 2013; Henry et al., 2014; Johnson, n.d.; Moffat, 2015; Rojo Rodriguez & Mckenzie, n.d.; Stanger & Roe, 2007). Additionally, GPR's history of use in archaeology provides a robust framework for its deployment. This body of previous work increases the speed and ease of use of GPR in the field. However, GPR does have limitations that may affect its effectiveness at the sites discussed above. The presence of large amounts of buried metal can shield objects buried below it, for example buried reinforced concrete slabs (Billinger, 2009; Goodman & Piro, 2013; Moffat, 2015). Similarly, soils with high conductivity can also interrupt GPR surveys. Soils rich in clay or saturated with groundwater, particularly highly conductive ground water like those contaminated with metals can result in rapid attenuation of GPR waves (Burger et al., 2006). Subterranean conditions are not the only potential obstacles to GPR, as surface conditions can also interfere with GPR surveys. A GPR survey requires the antenna to be in constant contact with the ground, termed coupling, and be moved in transects that are as straight as possible. Objects on the surface, such as structures, vegetation, animal burrows, or any other obstructions can cause decoupling, where the antenna losses contact with the ground (Billinger, 2009; Conyers, 2006; Goodman & Piro, 2013; Moffat, 2015; Sanger et al., 2020).

Electrical resistivity tomography (ERT) also has an established history as a geophysical method used in archaeology. The use of ERT in cemetery settings relies on the variations in the resistive properties of the subsurface caused by features associated with burials. These variations are often related to changes in the groundwater or by the resistive properties of buried objects. Examples include changes in water saturation related to soils that have been disturbed by human activity, ground water or soil that has been enriched by decomposing organic material and buried objects; all of which can cause resistive anomalies (Moffat, 2015). ERT surveys require connected electrodes to be placed in good contact with the ground and thus can work well in uneven or vegetated areas which would create problems for GPR (Sanger et al., 2020). The limitations of ERT in cemetery applications are related to both subsurface conditions and the resolution of the method. ERT can have difficulty when being used in soil that has high conductivity. These conditions can result in the bulk of the energy being passed along shallow paths in the subsurface reducing the resolution with depth. Buried metal objects can also interfere with the path of the electrical current. Extremely desiccated soils may also limit ERT surveys, as many soils need moisture to be conductive. With no ability to conduct the electrical current the equipment will simply note the entire survey area as extremely resistive (Burger et al., 2006). The resolution of ERT surveys is dependent on the spacing of the probes, as is the depth of imaging. To maintain proper sensitivity at depth resolution must be sacrificed.

Conductivity is inversely related to resistivity, making it a measure of the grounds ability to pass an electrical current. Magnetic susceptibility is directly related to the magnetization of a material in relation to the strength of the magnetic field (Bigman, 2012; Burger et al., 2006; Sea

& Ernenwein, 2021). Conductivity's close relationship with resistivity makes electromagnetic induction (EMI) conductive data and ERT data good supplements to one another. The data sets share their utility for archaeologists to measure variations in the conductive properties of the subsurface with two distinct but linked attributes (Moffat, 2015; Sea & Ernenwein, 2021). Additionally, EMI instruments can be used to detect objects with high magnetic susceptibility such as buried metal objects or fired soils (Bigman, 2012; Moffat, 2015; Sea & Ernenwein, 2021). EMI surveys are less susceptible to surface obstacles because they do not require coupling with the ground and can allow one person to survey large areas relatively quickly. Like other geophysical methods which rely on electromagnetic energy, EMI can struggle if the ground conditions are either highly conductive or resistive or in the presence of strong electromagnetic fields (Burger et al., 2006; Moffat, 2015).

Magnetometry measures the magnetic field which is a result of the magnetic susceptibility of the subsurface. Magnetic susceptibility can be altered by changes in ground water, soil composition, or buried objects (Bevan, 2017; Bullion et al., 2022; Juerges et al., 2010; Moffat, 2015). The ability to detect elevated iron levels in the subsurface can be useful in locating soils impacted by human activity, including burials. Additionally, concentrations of organic material or variations in ground water caused by soil disturbances can cause magnetic anomalies (Bevan, 2017; Bullion et al., 2022; Moffat, 2015). These properties allow the method the potential to locate both buried materials as well as grave shafts. Magnetometry is less susceptible to extreme levels of saturation of ground water as both high and low-water tables still provide useful data, and the system can detect magnetic anomalies even in electrically conductive soils that can interfere with electrical methods. However, magnetometry can be sensitive to powerful electromagnetic fields, such as powerlines, which can overwhelm the sensor making data collection difficult (Moffat, 2015).

Table 1:Geophysical instruments used at each site listed with the advantages and disadvantages for each.

Geophysical Instruments Deployed				
Method	Active/Passive	Sites Investigated	Pros	Cons
Ground-Penetrating Radar (GPR)	Active	Gould Community Center, Evangelical Lutheran Cemetery, Kingston Cemetery	- Common method that has shown replicable results in cemetery settings. - Can detect both magnetic and non-magnetic materials. - Both buried objects and soil disturbances are detectible with this method.	- Difficult to maneuver around surface obstacles. - Buried metal or other extreme changes in the electric properties in the shallow subsurface can block deeper imaging. - Waves can be attenuated by conductive soils.
Electrical Resistivity Topography (ERT)	Active	Gould Community Center and Evangelical Lutheran Cemetery	- Can easily be deployed around surface obstacles. - Changes in the resistivity of the subsurface can be related to both buried objects and soil disturbances. - Detects changes in ground water concentration which are often related to disturbances in the subsurface.	- Resolution is dependent on sensor spacing and is consistently lower than other methods. - Extreme soil conductivity makes data collection impossible.
Electromagnetic Induction (EMI)	Active	Evangelical Lutheran Cemetery and Kingston Cemetery	- Can easily be deployed around surface obstacles. - Both magnetic and electrical anomalies are investigated. - Like resistivity, conductivity is excellent for monitoring changes in ground water.	- Susceptible to extremes in soil conductivity. - More dependent on ground water than other electrical methods. - Difficult to determine depth of anomalies.
Magnetometry	Passive	Evangelical Lutheran Cemetery and Kingston Cemetery	- Can detect magnetic changes caused by soil disturbances, soil chemistry, and buried objects. - Less affected by extremes in soil conductivity. - Excellent at detecting ferro-magnetic material.	- Magnetic fields unrelated to the subsurface can interfere, for example power lines. - Difficult to determine depth of anomalies.

Chapter 3: Methods

In this section I will describe the archeological methods used to investigate potential unmarked human burials at the Gould Community Center, Kingston Cemetery, and Evangelical Lutheran Cemetery. Geophysical techniques were the only methods deployed for this thesis because they offer the least invasive approaches available in locating unmarked burials. I processed, analyzed, and interpreted the GPR, ERT, EMI, and magnetometry data using software at the CRAG laboratory at Colorado State University. I reviewed past research done on cemetery locales to determine which of these methods should be prioritized and balanced this information with the equipment I had available. GPR has an established history of use in cemetery contexts and was employed at all three sites (Conyers, 2006; Goodman & Piro, 2013; Henry et al., 2014; Moffat, 2015). I conducted ERT surveys at both the Gould Community Center and Evangelical Lutheran Cemetery. EMI and magnetometry surveys were completed for both Kingston and Evangelical Lutheran Cemeteries. Integrating these different geophysical results allowed a more thorough understanding of the subsurface and provided insight into which areas of these sites may contain unmarked burials.

Before I initiated data collection with geophysical instruments, I established global positioning system (GPS) base stations using Carlson BRx6+ GNSS receivers. To establish a site datum, I used multi-hour static data collection that I processed using the OPUS correction available through NOAA. This allowed me to use a GPS base station and rover to situate the geophysical data that I collected within the real world. The data was then processed using various software suites including GPR-Slice, RES2DINV, TerraSurveyor, Surfer, and DAT38 MK2. Finally, fully processed data were visualized as raster datasets in ArcGIS Pro where I compare across all data sets to identify and interpret subsurface patterns.

Ground-Penetrating Radar (GPR)

Ground-penetrating radar is an active method of near surface geophysics, meaning it sends a signal into the ground and measures the results of that signal interacting with the subsurface. The signal used by GPR comes in the form of electromagnetic energy which is emitted into the ground as radio waves that reflect as they interact with variations in the subsurface. Through measuring these reflections, the technology can detect buried objects and changes in soil stratigraphy (Burger et al., 2006; Conyers, 2006; Moffat, 2015). The reflection, refraction, and attenuation of a wave of electromagnetic energy depends on the contrast between the electrical properties of any two given materials as the wave passes from one material to the other. The greater the contrast, the more energy from the wave will be reflected to the antenna (Goodman & Piro, 2013). The specific electrical property that is measured by GPR is the dielectric constant of the material (Burger et al., 2006). The dielectric constant of a material is related to the materials ability to hold an electrical charge. As the dielectric properties change the speed of an electromagnetic wave passing through it changes. The relationship between the speed of the wave and the dielectric constant is represented by the equation,

$$v = \frac{C}{\sqrt{\varepsilon}}$$

where v is the velocity of the wave ε is the dielectric constant and c is the speed of light in vacuum (Burger et al., 2006; Goodman & Piro, 2013). The speed of light constant is also the speed of radio waves as they move through a vacuum. The energy of the electromagnetic wave emitted into the ground will dissipate the further it travels; this is what is meant by the attenuation of the wave. The rate that the radio waves attenuate is primarily controlled by the conductivity of the material that they are travelling through as conductivity is directly related to the dielectric constant. The more conductive a material is the higher its dielectric constant is, this means that more conductive materials will act as capacitors and absorb the energy of the wave. The higher the conductivity the more rapid the attenuation of the wave, and the less depth can be imaged (Goodman & Piro, 2013). This means that highly conductive materials will have limited to no transmission of electromagnetic waves passing from materials with lower conductivity. Metal objects that are buried in the ground reflect all the electromagnetic energy back once contact with the surface of the object is made. Since metal is extremely conductive compared to the surrounding material the majority of wave's energy is reflected. This means that GPR cannot penetrate metal, it may only detect the surface of a metal object (Burger et al., 2006; Conyers, 2006; Goodman & Piro, 2013).

I used the GSSI's SIR-4000 GPR system with the 350 MHz hyperstacking shielded antenna provided by the CRAG laboratory at Colorado State University. The SIR-4000 system follows the basic layout of most GPR units with a computer, an antenna, and a power source operated as one system. The system can be deployed with just a survey wheel attached to the antenna or with a full three wheeled carriage system. The survey wheel set up requires a harness for the computer and power source to be carried by the operator. The carriage holds the computer unit while the power source is held within a harness, but the antenna is placed in a plastic tub that is meant to be in constant contact with the ground. When using the system in either configuration the survey is conducted by moving the antenna across the ground in transects forming a grid. The device collects reflection data for the length of the transect at set intervals and these transects are processed into cross-section images of the ground (Goodman & Piro, 2013). Completing transects in a grid ensure that the subsurface is imaged in a way that can be processed into two- and three-dimensional images. The radio waves that are emitted into the subsurface interact with changes in the soil and buried objects where portions of the wave will reflect, refract, or attenuated in the subsurface (Burger et al., 2006; Conyers, 2006; Goodman & Piro, 2013). These changes in the subsurface can be used to identify anomalies in the subsurface that could relate to unmarked burials (Moffat, 2015). These anomalies can be visualized in both two and three-dimensional graphical representations. I processed the data collected using Geophysical Archaeometry Laboratory's GPR-Slice MT software. With this software I applied a time 0 correction and background filter, followed by a migration filter to the radargrams.

The GPR surveys I conducted at the three sites differed in scale and in the use of the carriage provided with the SIR-4000. The survey I conducted at the Gould Community Center was the smallest in scale and was done with the survey wheel attachment to record the transect lengths. The Gould survey was done as two single lines, each following a portion of the ERT lines that I also collected during my research at the site (Figure 6). Additionally, I collected a 2 x 4 m grid, with 50 cm transects, at the Gould Community Center. The time window was set to 40 ns and the samples per scan was 512. The forest cover at the site made the deployment of GPR difficult, as a result I prioritized covering portions of the ERT survey. This resulted in the collection of two GPR tracts on the western part of the ERT lines and the collection of a grid near a standing concrete marker that was in a unforested portion of the survey area. The north side of the marker where the grid was collected was chosen using the ERT data, which located a resistive anomaly. Additionally, the south side gradually sloped down and dropped off into the nearby floodplain of the Michigan River. To complete the surveys at Kingston and Evangelical Lutheran Cemeteries, I used the carriage system designed for the SIR-4000. At Kingston Cemetery the data collection was done with two separate grids sized 40 x 70 m with transects spaced 50 cm apart. The time window was set to 40 ns and the samples per scan was 1024, however the grids are further separated due to the system resetting to 512 samples per scan when the battery was swapped out. As a result, I have four separate GPR grids collected for Kingston Cemetery. The two western grids were collected at 1024 and the two eastern grids were collected with 512 samples per scan. I collected data at Evangelical Lutheran Cemetery in two grids, one sized 20 x 40 m and the other 20 x 30 m, both with 50 cm transect spacings. The time window was set to 40 ns and the samples per scan was 512. I used the GPR-Slice software to grid these data sets together.

Electrical Resistivity Tomography (ERT)

Electrical resistivity tomography (ERT) is another active method used in geophysical investigations. ERT passes electricity into the subsurface to measure variations in the electrical resistivity of the ground, measured in Ohm/m. This relationship is represented in its simplest form by Ohm's Law which can be shown with the equation,

$$i = \frac{V}{R}$$

where the electric current, *i,* is directly proportional to the voltage, *V*, and inversely proportional to the resistance, *R* (Burger et al., 2006). The equipment needed to complete an ERT survey includes a power source, cables, electrodes, and a computer which is used to collect the data (Burger et al., 2006). The survey is conducted by inserting an array of electrodes into the topsoil, typically no deeper than 20cm, and passing a series of electrical currents through the ground between varying sets of electrodes. Generally, the electrode spacing affects the survey depth, with longer surveys penetrating deeper into the subsurface (Burger et al., 2006). An ERT survey passes current from a source electrode to a sink electrode as the voltage between two potential electrodes is measured. Thus, an ERT survey with several electrodes allows for voltage to be measured at any two given electrodes along the profile. The resistivity is then calculated from the measured voltage and known current. Apparent resistivity is the term for the resistivity measured during an ERT survey (Burger et al., 2006). The subsurface is assumed to be nonhomogeneous and thus the apparent resistivity between electrodes is an average for the material that separates any two electrodes (Burger et al., 2006; Doro et al., 2022; Moffat, 2015).

I used the SYSCAL Pro system loaned to me for this project by the Colorado State University Department of Geosciences. This system uses 48 electrodes connected by 4 cables to a control box, the system is powered either by an internal power source or a twelve-volt external power source. The inversion software I used to construct resistivity models is called RES2DINV. The software compiles the data from each set of electrodes and uses this to show the user where resistive lows and highs may reside in the subsurface. The resolution of the data and thus the inversion model depends on both the spacing of the electrodes and the number of electrodes deployed. Resistive or conductive anomalies shown by the inversion models may be caused by several ground conditions including variations in the porosity or mineral composition of the subsurface, changes in the groundwater chemistry or concentration, or buried objects (Henry et al., 2014; Moffat, 2015).

I surveyed both the Gould Community Center and Evangelical Lutheran Cemetery using ERT. Due to limited time with the ERT equipment I was unable to integrate this method at Kingston Cemetery. ERT surveys were organized as Dipole-Dipole arrays that were arranged with 1 m spacing between the electrodes to increase near surface resolution without sacrificing resolution at depths up to 2 m. I deployed two lines measuring 48 m at the Gould Community Center, these lines were placed to transect as many concrete markers as possible. This resulted in lines that were not parallel and were spaced between one meter, at the western end, and approximately 10 meters apart, at the eastern end (Figure 5). There are various toppled concrete markers in the shape of stele scattered across the site where only one is left standing. At Evangelical Lutheran Cemetery five roll along lines measuring 72 m were positioned with the first electrode in the south and the final one in the north (Figure 10). The survey was designed to evenly sample the 20 m width of the cemetery while intersecting as many marked burials as possible. I placed the first line on the western edge of the cemetery, the second line four meters east of that, the third line was placed six and half meters east of the second, the fourth was another four meters east of the third, and the fifth line was the furthest east four meters from the fourth line.

Electromagnetic Induction (EMI)

Electromagnetic induction is another active geophysical method I used to survey for unmarked burials. EMI measures variations in both the conductivity, measured in milli siemens per a meter (mS/m), and magnetic susceptibility, measured in parts per a thousand (ppt), of the subsurface by inducing secondary electromagnetic fields in conductors within the ground (Burger et al., 2006; Moffat, 2015; Sea & Ernenwein, 2021). This can be described with Faraday's Law, which is represented by the equation,

$$curlE = -\frac{\partial B}{\partial t}$$

Where an electric field E is produced by a changing magnetic field, B, over a change in time, t. Magnetic fields are also produced by changing electrical fields as described in Ampere's Law, which is represented by the equation,

$$curlH = \frac{\partial D}{\partial t} + I$$

where H is the magnetic field, D is the electric field displacement, t represents time and I is the current density, which is directly related to electric conductivity (Burger et al., 2006). By passing an alternating current (AC) through a coil or transmitter, a magnetic field can be generated, AC is used since changing electric fields are needed to produce an alternating magnetic field, this magnetic field, called the primary field, produces voltage in the receiver set some distance from the transmitter within the same device. The distance between the transmitter and the receiver controls the depth that the device will image (Moffat, 2015). Additionally, EMI instruments can be used to detect objects with high magnetic susceptibility such as buried metal objects or fired soils (Moffat, 2015; Sea & Ernenwein, 2021). Similar to ERT, EMI does not require coupling with the ground but is limited by subsurface conditions that are either very conductive or resistive.

I used the EM38-MK2 system from Geonics Ltd. to collect electromagnetic data. This system uses two sensor spacings, one at 50 cm and another at 1 m. I used this system at Kingston and Evangelical Lutheran Cemeteries. I collected data in two 40 x 70 m grids separated into north and south grids. At Kingston Cemetery I used the manual mode, which requires the user to trigger the instrument to collect data at set intervals, to collect data every 1 m with a transect spacing of 50 cm. The system was set to 5 readings per a second, which corresponded to one press of the manual trigger in this survey. The transects were collected in alternating directions with the first line going west to east. To collect data at Evangelical Lutheran Cemetery I utilized an attached Carlson BRx6+ GNSS GPS set up as a rover, connected to the sites GPS base station, and enabled auto mode on the EM38 MK2 to collect data without the need to follow a set grid. I used the 5-sensor cart designed for the SENSYS magnetometer to suspend the EM38 MK2 below the GPS rover. The system allowed the rover to be positioned above the center of the instrument while remaining far enough away to avoid interference. The instrument was set to take 5 samples per a second and a 1 m spacing was used on the transects as the spacing of the wheels was used by the operator as a guide. I used DAT38 MK2 program to transform the raw N38 files to M38 files. I then brought these files into TerraSurveyor software for the data collected at Kingston Cemetery while the GPS tagged data from Evangelical Lutheran Cemetery was brought into the Surfer software for processing. In TerraSurveyor I applied a despiking function to remove extreme values from both the conductivity and magnetic susceptibility data. I then applied a 3 x 3 Gaussian low pass filter to the data and the edge matching feature to create a more continuous visualization between the two grids collected at Kingston Cemetery. I applied a kriging interpolation in Surfer while griding the GPS tagged data from Evangelical Lutheran Cemetery to address any overlapping in the data. I then applied a 3 x 3 Gaussian low pass filter to remove low frequency noise from the data.

Magnetometry

Magnetometry is the only passive geophysical technique I used in my data collection. It is considered passive as it does not send any signal into the ground, instead variations in the naturally occurring magnetic field is recorded. In the case of magnetometry the variations in the Earth's magnetic field are measured in nanoteslas (nT) (Bevan, 2017; Burger et al., 2006). These variations are caused by changes in the magnetic susceptibility of the subsurface. This is the same physical property being investigated by EMI, however magnetometry measures the magnetization caused by the Earth's magnetic field rather than one produced by the instrument itself. The relationship between magnetization and magnetic susceptibility is represented by the equation,

$$l=kH$$

where l is the magnitude of the magnetization, k is the magnetic susceptibility, and H is the intensity of the magnetic field (Burger et al., 2006). The Earth's magnetic field varies naturally between the equator and the poles. The strength of the magnetic field at the equator is approximately 30,000 nT while the strength at the poles is around 65,000 nT. With the strength of the Earth's magnetic field being a known constant, changes in the magnitude of the magnetization and magnetic susceptibility of a material can be calculated (Bevan, 2017; Henry et al., 2014; Juerges et al., 2010). Passing two magnetometers with a known vertical distance between them over the surface allows variations in the magnetic field to be observed.

I used the SENSYS MAGNETO MXPDA system with five gradiometers spaced 25 cm apart to collect magnetometry data. I deployed this method at both Kingston and Evangelical Lutheran Cemeteries. I used the Carlson BRx6+ GNSS rover attached to the magnetometry cart to geolocate the data collected. This allowed for 25 cm transects with minimal spacing or overlap between passes with the cart. Overlap was filtered out of the data using the kriging interpolation tool available in the Surfer software. I collected the magnetometry data at both cemeteries in the north-south direction, perpendicular to the orientations of the known burials at the site. Data collected by the MAGNETO MXPDA system is displayed as a magnetic gradient which displays the variations in the magnetic field over a horizontal area. This data was processed by applying a zero-median filter with a 5 m moving window to the data in the MAGNETO software. This filtered data was then pulled into Surfer where I gridded the data.

Chapter 4: Results

Gould Community Center

Both GPR and ERT were deployed to survey the Gould Community Center (Figure 5 and 6). EMI and magnetometry data were not collected at the Gould site due to limited evidence for extant burials. I collected ERT data at the Gould Community Center on August 11, 2021. The results of the ERT data were analyzed after they had been run through an inversion and modelling program called RES2DINV. The resulting ERT inversion models had RMS errors of 2.5% and 3.5% respectively. Both lines show layering in the resistive properties of the subsurface, this is especially apparent in the inversion model of line two (G-E-2) (Figure 7). I interpret two geoelectric layers in the models, a shallow layer with lower apparent resistivity and a deeper layer which has a higher apparent resistivity. At this site, the low range is 300-1500 ohm/m, while the high range is 1500-2400 ohm/m (Figure 7). This layering can be seen in both lines, but line one (G-E-1) is significantly more resistive in the shallow layer than line two (G-E-2). Line one (G-E-1) shows several shallow resistive anomalies that disrupt the layered pattern of the model possibly associated with disturbances in the soil stratigraphy. The results also show a series of large resistive anomalies present in both lines, one of these corresponds to the standing surface marker (Figure 7).

Figure 5: Locations of ERT Line 1 (G-E-1) and Line 2 (G-E-2) in the survey area near the Gould Community Center.

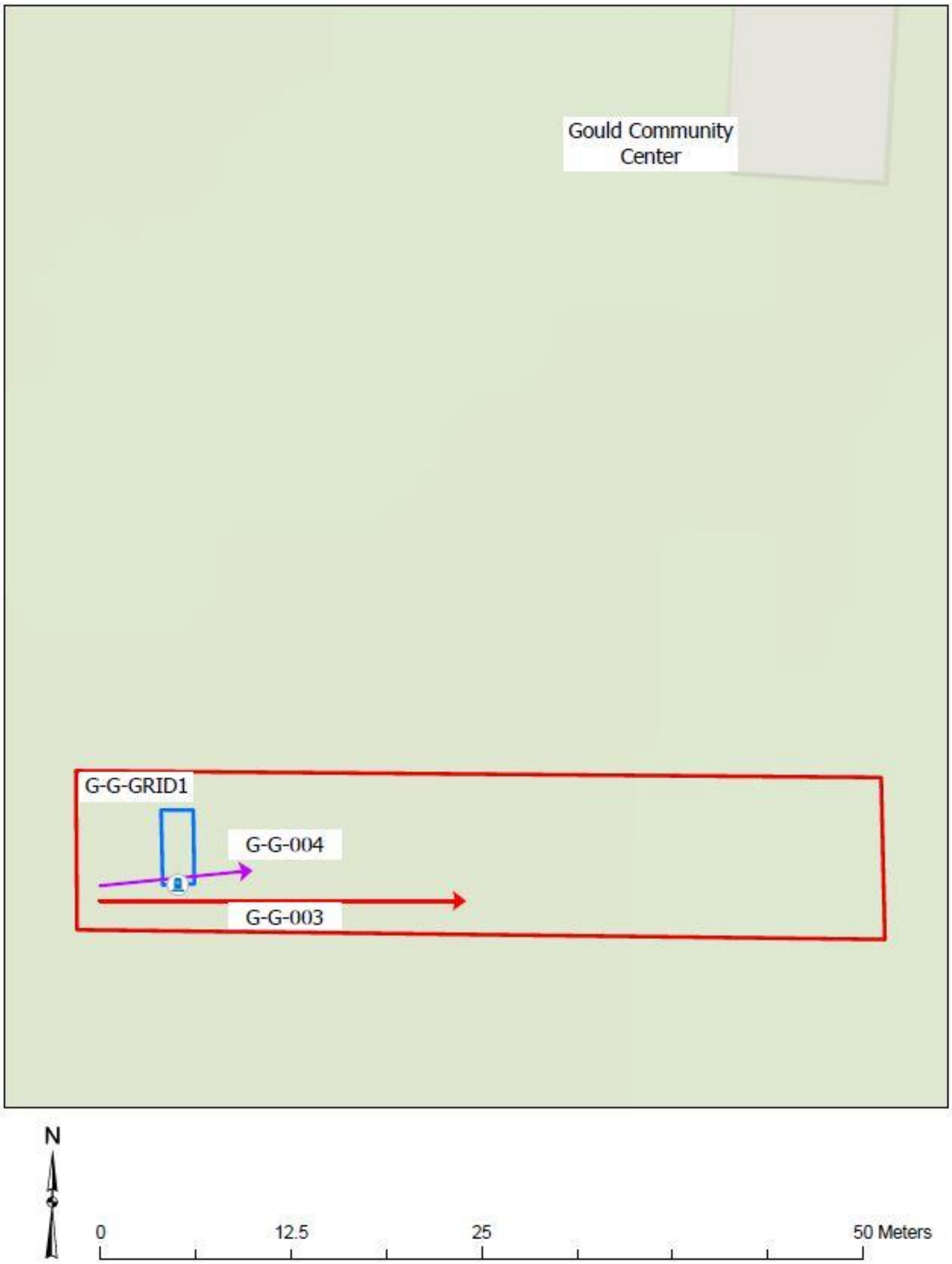

Figure 6: Locations of the GPR grid (G-G-GRID1) as well as lines 3 (G-G-003) and 4 (G-G-004) in the survey area near the Gould Community Center.

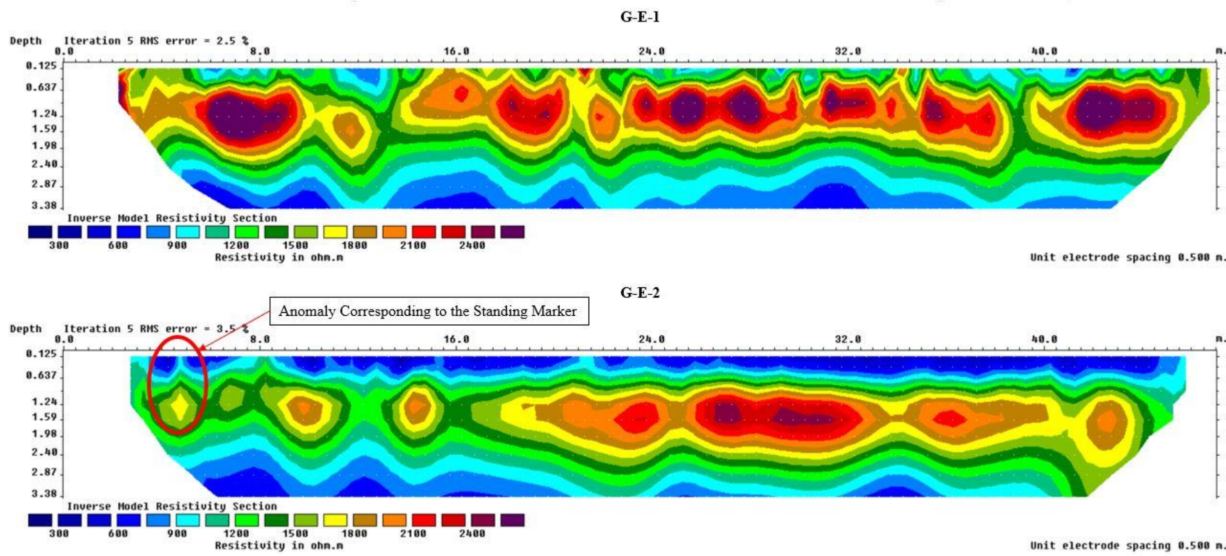

Figure 7: G-E-1 and G-E-2 from the survey of the Gould Community Center.

Radargrams from the GPR lines followed the same path as the ERT lines extending along the western 10 m of G-E-1 and the western 24 m of G-E-2. The small resistive anomaly between the 4 m and 6 m mark visible on G-E-2 was the target of the 2 x 4 m GPR grid (G-G-GRID1) collected near the standing concrete marker (Figure 7). I collected the GPR data on August 12, 2021. I used GPR-Slice to generate a composite grid and identified a high amplitude reflector that correlates with the position on G-E-2 at a depth slice of around 75 cm (Figure 8). There are several weak reflectors seen in both the gridded model and the individual radargrams that appear layered. Reflectors are between 1 and 4 m in size and overlay each other forming the layered appearance previously discussed (Figures 8 and 9).

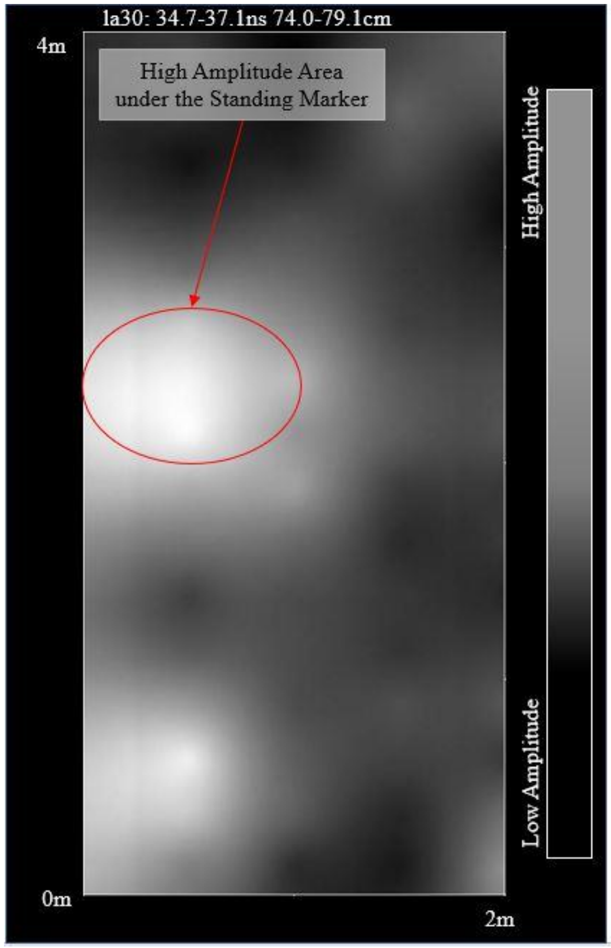

Figure 8: GPR Slice from approximately 75 cm near the standing marker at the Gould Community Center. Created using gridded data from G-G-GRID1.

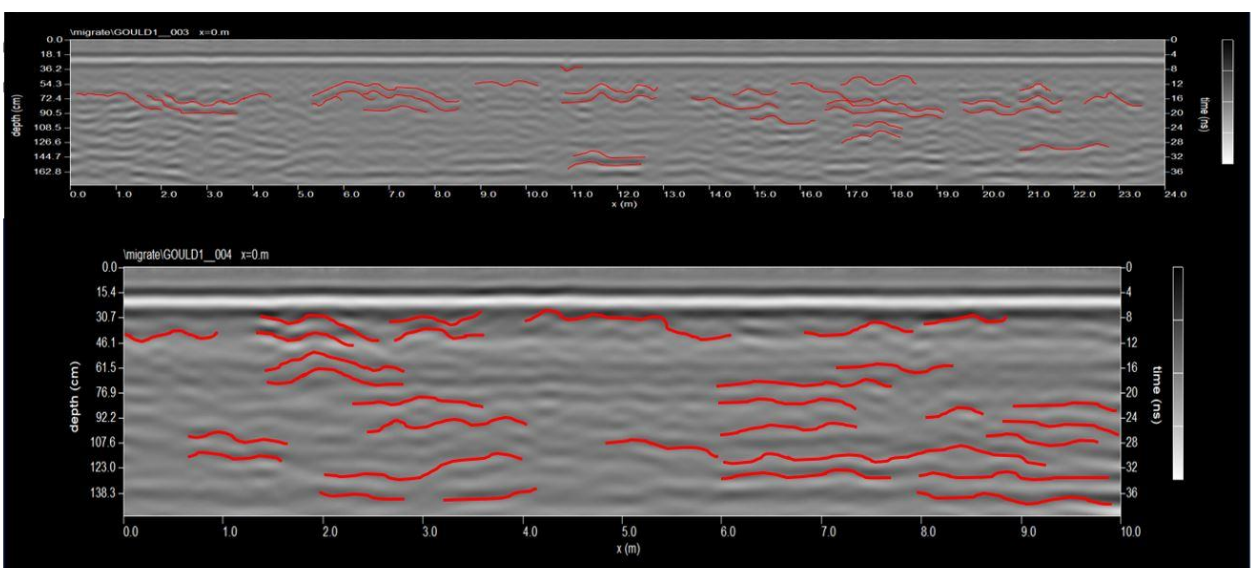

Figure 9: Radargrams from Gould GPR lines labeled 003 (G-G-003) and 004 (G-G-004) with reflectors highlighted by author.

Evangelical Lutheran Cemetery

GPR, ERT, Magnetometry, and EMI were used to survey Evangelical Lutheran Cemetery. This allows comparison of the results from the four methods. The portions of the cemetery with marked burials were surveyed at the same time as the unmarked areas, a total area of approximately 20 x 70 m, to allow comparisons between known burials and potential unmarked burials. Five ERT lines were collected from the Evangelical Lutheran Cemetery (see Figure 10). I was assisted in the collection of the ERT data by a graduate student from the geology department at Colorado State University on August 4, 2021 and August 5, 2021. The RMS error for the five roll-along lines collected ranged from 8.3% to 10.3% (Figures 11 and 12). All five lines show two geoelectric layers with anomalies periodically interrupting the layering. The shallow layer has a higher apparent resistivity and increases in thickness as the lines extend north. The low range of resistivity at this site is 10-63 ohm/m, while the high range is 63-254 ohm/m (Figures 11 and 12). This layer is between 50 and 200 cm thick across the site. Numerous small resistive anomalies can also be seen in this layer. The deeper layer has a lower apparent resistivity and extends to the maximum depth imaged by the model (Figures 11 and 12).

Figure 10: Locations of the five ERT lines collected at Evangelical Lutheran Cemetery.

Line one shows resistive layering in the model with the shallow layer having a relatively uniform thickness, at around 50 cm, in the southern 50 m of the line (Figure 11). There are numerous small anomalies present in the shallow layer, these are most prevalent in the southern half. Additionally, line one shows an increase in the thickness of the layer of higher apparent resistivity from approximately 50 to 200 cm on the northern 20 meters (Figure 11). Line two has a shallow layer of higher apparent resistivity with an approximate thickness of 50 cm and multiple anomalies in the southern 50 m of the line (Figure 11). The northern portion of line two is dominated by a large area of high apparent resistivity that expands to around 200 cm (Figure 11). Additionally, between 10 and 11 meters north of the first electrode there is an area of low apparent resistivity that is modeled as a disturbance in the resistive layers and reaches a depth of more than 300 cm. Line three has a comparable layer thickness, as well as the intermittent anomalies in the shallow layer, as that seen in lines one and two (Figure 12). However, the large area of higher apparent resistivity on the northern half of line three extends from approximately 44 m north of the first electrode to the end of the line and expands to a depth of around 250 cm (Figure 12). Line four and line five continue the trend of a shallow layer of higher apparent resistivity that expands in the northern portion of the line (Figure 12). The expanded shallow layer of higher apparent resistivity on both lines four and five reaches from around 36 m north of the first electrode to the end of their respective lines and has a depth of around 250 cm (Figure 12). The lines are in order from west to east, with line one being the furthest west and line five representing the eastern line. The lines all have their first electrode in the south with the line running north 72 m (Figure 10). When taken together, the lines show that the southern half of the survey area has a thinner layer of higher apparent resistivity than the northern half, with expanded thickness in the northeast.

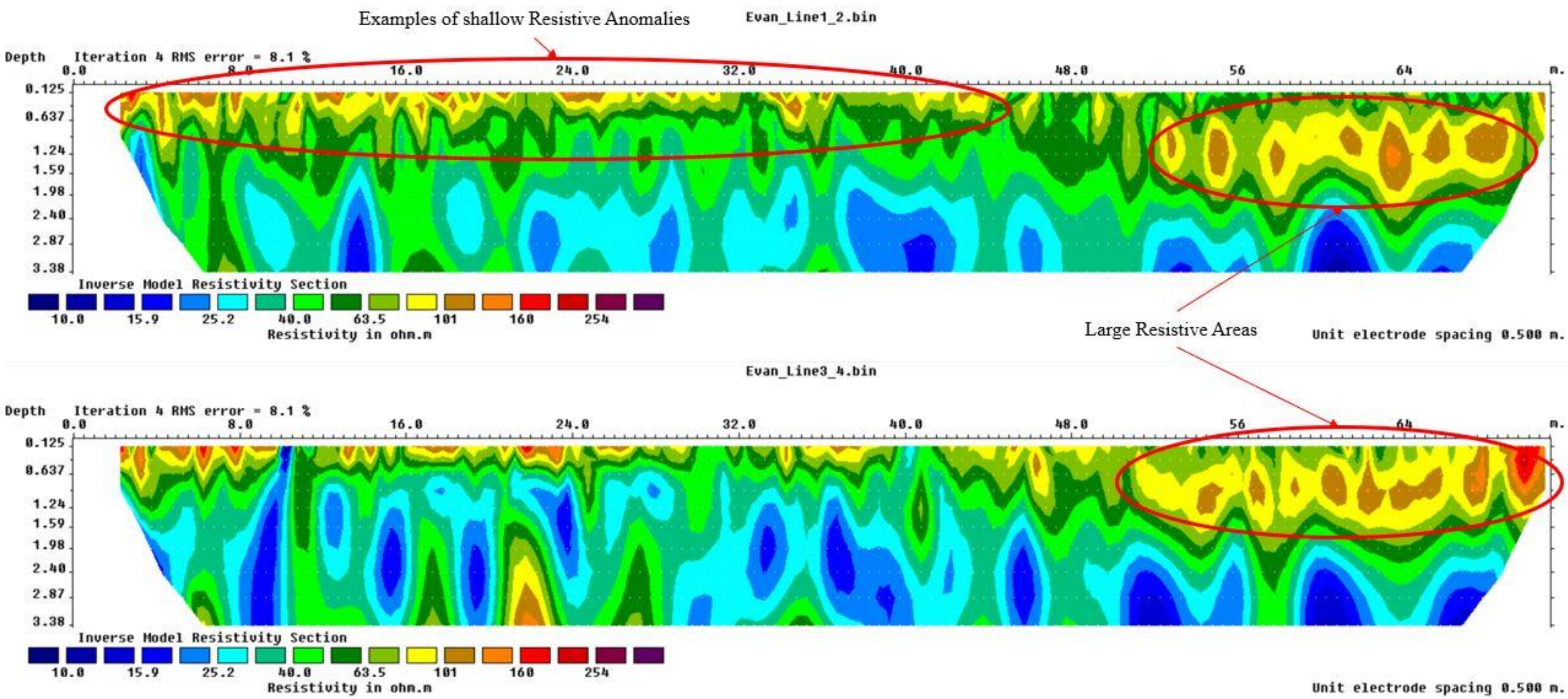

Figure 11: Line 1, (1_2) and Line 2 (3_4) at Evangelical Lutheran Cemetery showing examples of the shallow resistive anomalies seen near the surface in the southern parts of the lines as well as the resistive areas found in the northern part of the lines.

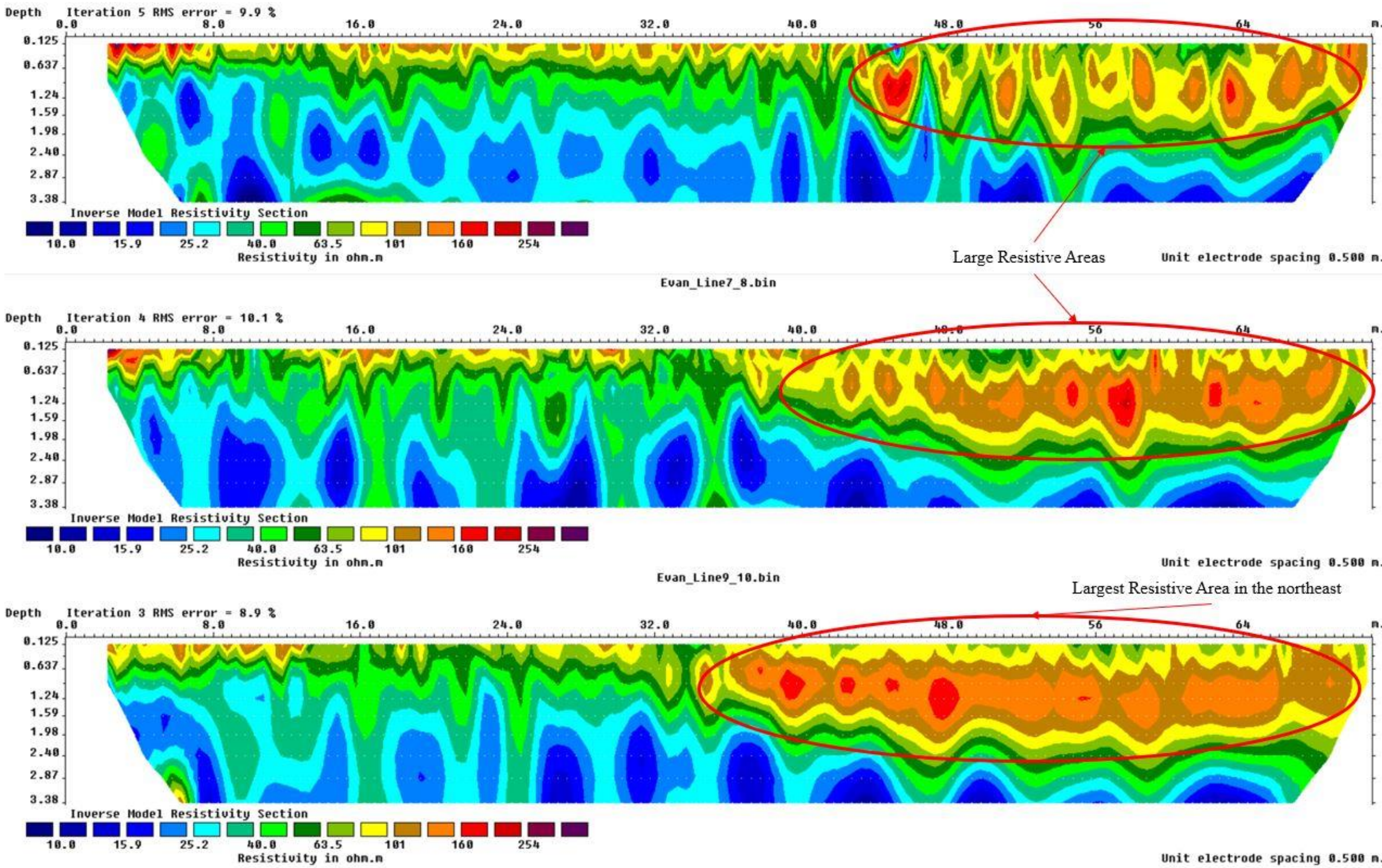

Figure 12: Lines 3 (5_6), 4 (7_8), and 5 (9_10) showing the expansion of the resistive area in north on the lines collected further to the east at Evangelical Lutheran Cemetery.

The radargrams from both grids collected at Evangelical Lutheran Cemetery were used to create a composite two-dimensional GPR image at a depth of approximately 1 m (Figure 13). The GPR data was collected with help from employees of the EYCCB on both August 19, 2021 and August 20, 2021. The northern grid shows linear noise resulting from its combination with the southern grid. The noise is amplified by the contrasts between the reflectors in the two data sets. The southern grid has stronger and more numerous anomalies causing the northern grid to appear exaggerated. The several groups of anomalies present are mostly located near known grave markers. Twelve of the fourteen marked anomalies occur in the southern part of the cemetery where the grave markers are present. The anomalies that are highlighted correspond to reflectors seen in the radargrams that were used to build the depth slice image (Figure 13). Of note is a group of anomalies in the southwest corner which appear adjacent to the known markers in that area (Figure 13). These high amplitude reflections can be seen in the corresponding radargram, which are highlighted as an example of the type of reflectors used to determine anomalies on the depth slice image (Figure 14). There are anomalies isolated from the known markers in northeast of the survey area. The first is 10 m south of the northern boundary and is visible along the eastern boundary. The second is around 15 m south of the northern boundary and 5 m west of the eastern boundary (Figure 13). Four of the southern anomalies appear isolated from known markers. The first is in the south on the boundary of the survey area around 6 m east of the southwest corner. The second is around 13 m north of the southern boundary and 2 m west of the eastern boundary. The third is 45 m north of the southern boundary and 2 m east of the western boundary. The final anomaly is around 45 m north of the southern boundary and 10 m east of the western boundary (Figure 13). Isolated was determined as there being more than 2 m between the anomaly and the nearest marker.

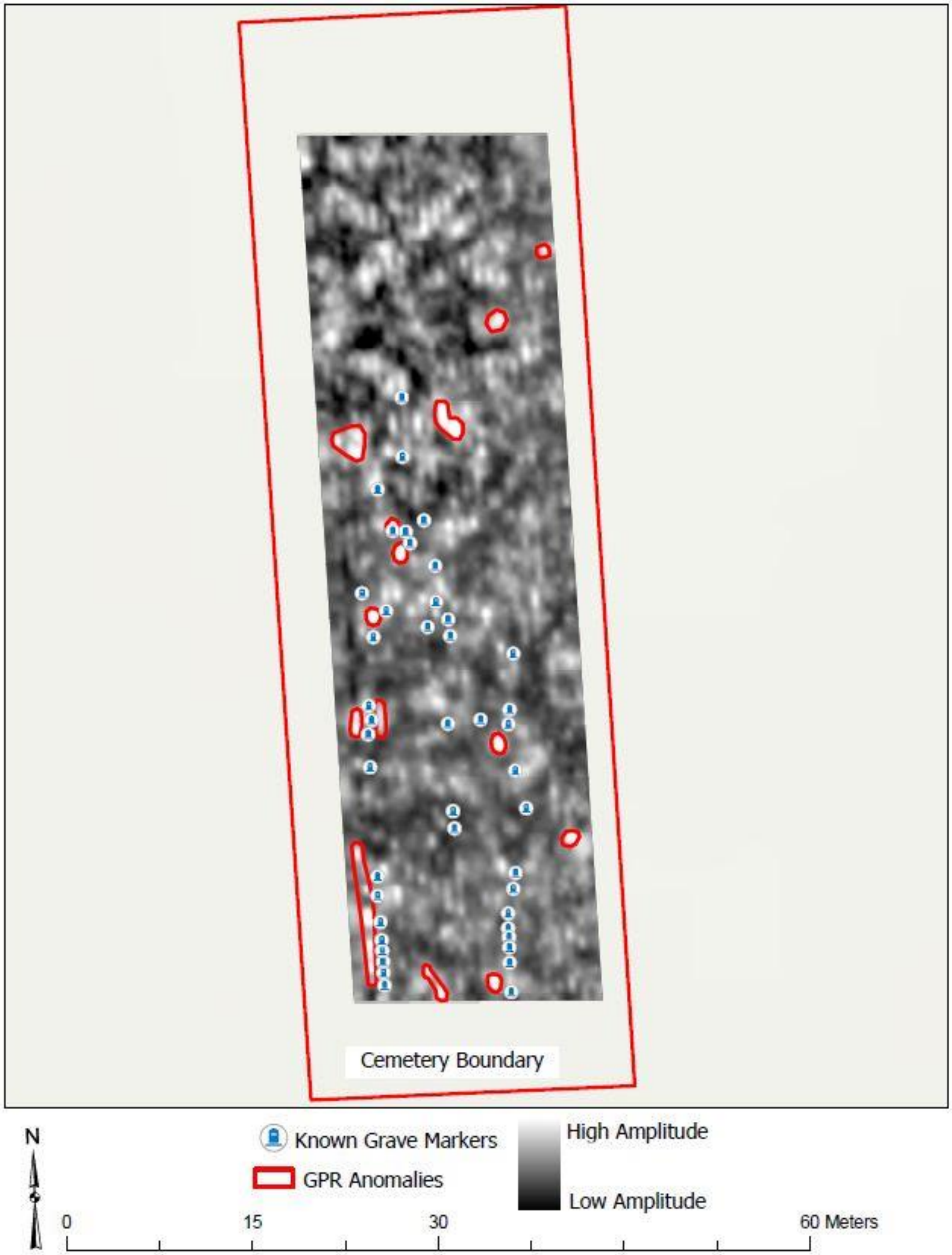

Figure 13: Gridded GPR results at Evangelical Lutheran Cemetery with anomalies and markers highlighted.

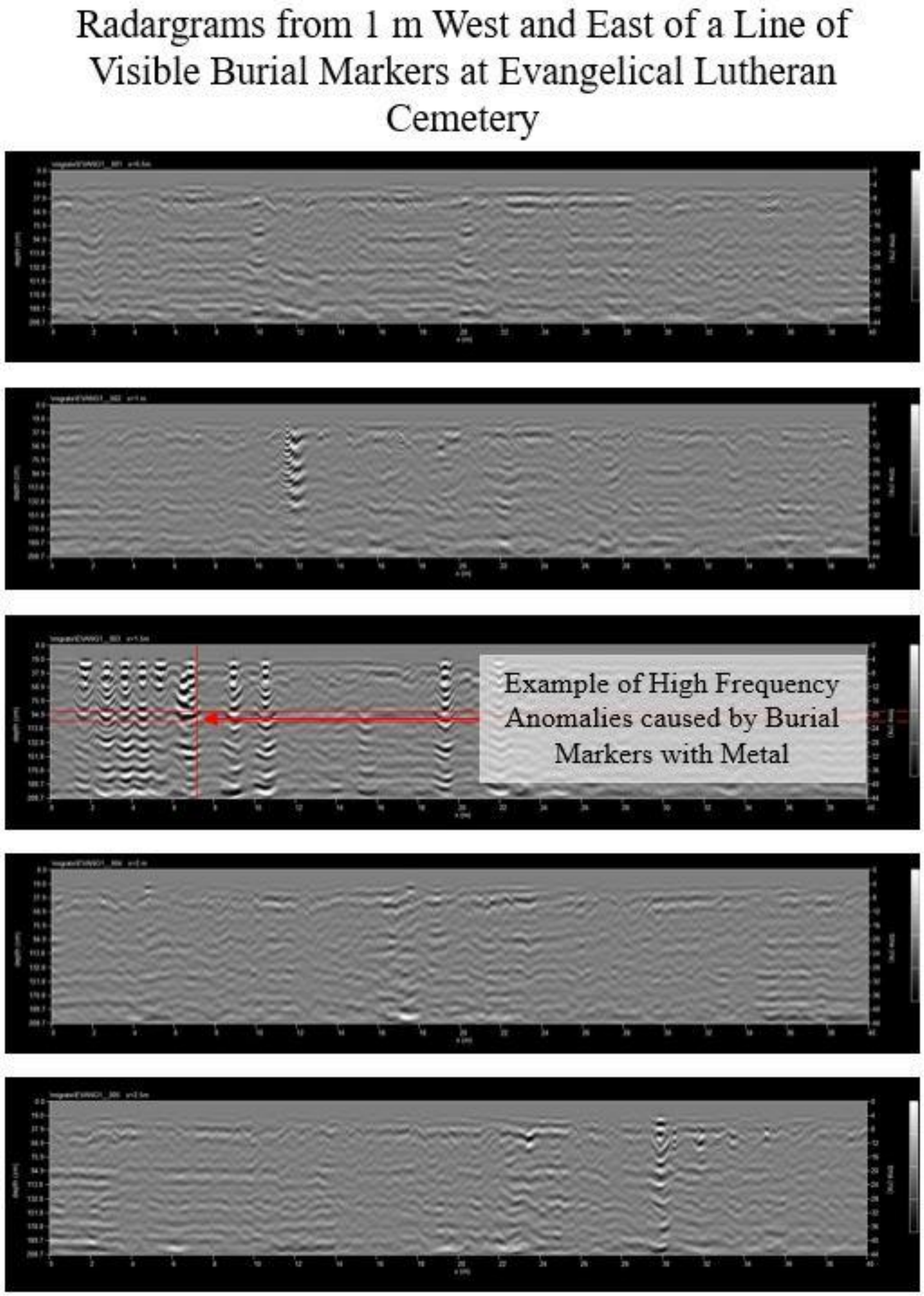

Figure 14: Radargrams in the southwest of Evangelical Lutheran Cemetery, these include radargrams from 1m to the east and west of known markers.

Magnetometry data was collected in one large grid at this site and the data was processed as such. I collected magnetometry data on June 2, 2022. Multiple anomalies were identified and separated into 8 groups based on relative proximity, known sources of noise, and intensity (Figure 15). The first group is visible as the large black anomaly along the southern edge of the survey area (shown in red in Figure 15). This area is closest to the overhead power lines that are located directly above the southern boundary of the cemetery. Group two represents two linear groups extending from the south to the north as a series of anomalies. One is approximately 1 m east of the southwest corner of the survey area and the second is around 10 m further east of the first (shown in blue in Figure 15). These features extend around 10 to 12 m from the northern boundary of group one toward the north. Group three consists of the anomalies centered around 10 m east of the western boundary and 20 m north of the southern boundary of the survey area (shown in green in Figure 15). This group covers an approximate area of 3 x 5 m and consists of two distinct clusters of anomalies. Group four is a large spread of anomalies centered around 10 m east of the western boundary and 40 m north of the southern boundary (shown in yellow in Figure 15). This large group covers an area around 18 x 20 m in size and dominates the center of the survey area. The group consists of five clusters of anomalies that have been sorted together as this area has multiple metallic burial markers and the anomalies are generally spikes in the magnetic data. Group five is approximately 10 m north of group four and around 3 m east of the western boundary (shown in purple in Figure 15). This group consists of one large anomaly surrounded by multiple smaller anomalies covering an area of approximately 7 x 7 m. Group six appears as a single large anomaly and is in the northwest of the survey area around 60 m north of the southern boundary and extending from the western boundary around 5 m (shown in light blue in Figure 15). This anomaly covers a 5 x 5 m area that extends past the western boundary. Group seven represents the cluster of large anomalies in the northeast portion of the survey area (shown in orange in Figure 15). The group is approximately 18 m east of the western boundary and 60 m north of the southern boundary. This group covers around a 7 x 7 m area of the survey and is isolated from the other anomalies, the closest being a small anomaly around 5 m to the southwest. Group eight represents the scattered magnetic anomalies that are concentrated in the southeastern and western portions of the survey area (shown in lavender in Figure 15). The anomalies of group eight are separated out based on proximity and intensity, they generally represent lower intensity anomalies.

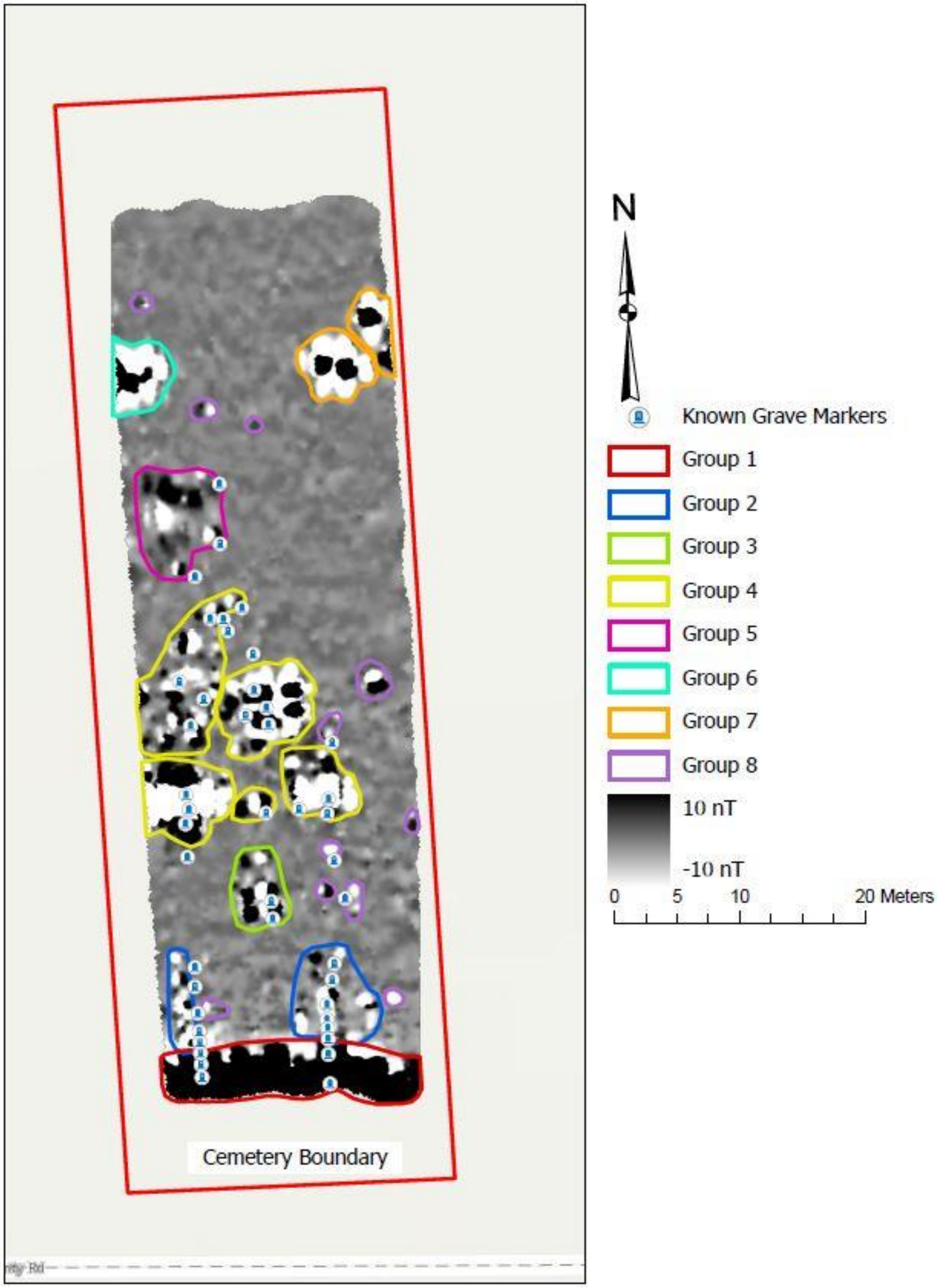

Figure 15: Results of the magnetometry survey at Evangelical Lutheran Cemetery with anomalies and markers highlighted. (The MXPDA system reports measurements in nT though the device measures the vertical magnetic gradient (nT/m). The vertical separation is 0.85 m.)

The EMI survey, collected as one grid, produced both conductivity and magnetic susceptibility data at two depths. However, the overlap in the data sets lead to only the conductivity data collected with a 50 cm sensor spacing being used for interpretation as that data set had the highest resolution. I conducted the EMI survey on June 2, 2022. Anomalies were divided into seven groups based on relative positions, intensity, and the presence of known features in the cemetery (Figure 16). Group one includes the two large anomalies on the southern boundary of the survey (shown in red in Figure 16). The eastern anomaly is approximately 3 x 5 m while the western anomaly is approximately 3 x 4 m in size. These anomalies are adjacent to a series of large metal posts in the southern portion of the cemetery as well as the overhead powerlines. Group two consists of the cluster of anomalies on the western boundary of the survey area, approximately 24 m north of the southern boundary of the survey area (shown in blue in Figure 16). The group is linear extending north to south and is approximately 3 x 13 m in size. Group three is centered approximately 9 m east of the western boundary and 34 m north of the southern boundary of the survey (shown in yellow in Figure 16). The area covered by group three is approximately 9 x 7 m. Group four is just to the north of group four, centered around 7 m east of the western boundary and 44 m north of the southern boundary of the survey (shown in pink in Figure 16). This grouping is approximately 7 x 10 m in size with two clusters of anomalies. Group five represents the northmost set of anomalies located along the eastern boundary of the survey (shown in green in Figure 16). The group is centered around 18 m east of the western boundary and 64 m north of the southern boundary and is around 4 x 7 m in size. Group five is isolated from other anomalies and represents the north most group of anomalies in the survey. Group six is centered around 14 m east of the western boundary and 28 m north of the southern boundary of the survey (shown in purple in Figure 16). This group is linear with a north-south orientation about 2 x 5 m in size. Group seven consists of scattered anomalies that are not included with the larger groups previously mentioned (shown in orange in Figure 16). These anomalies are generally smaller, the largest are 2 x 3 m in size, and are concentrated in the southern portions of the survey area near the burial markers. The anomalies of group seven are less common in the north where the burial markers are not present and are generally of a lower intensity.

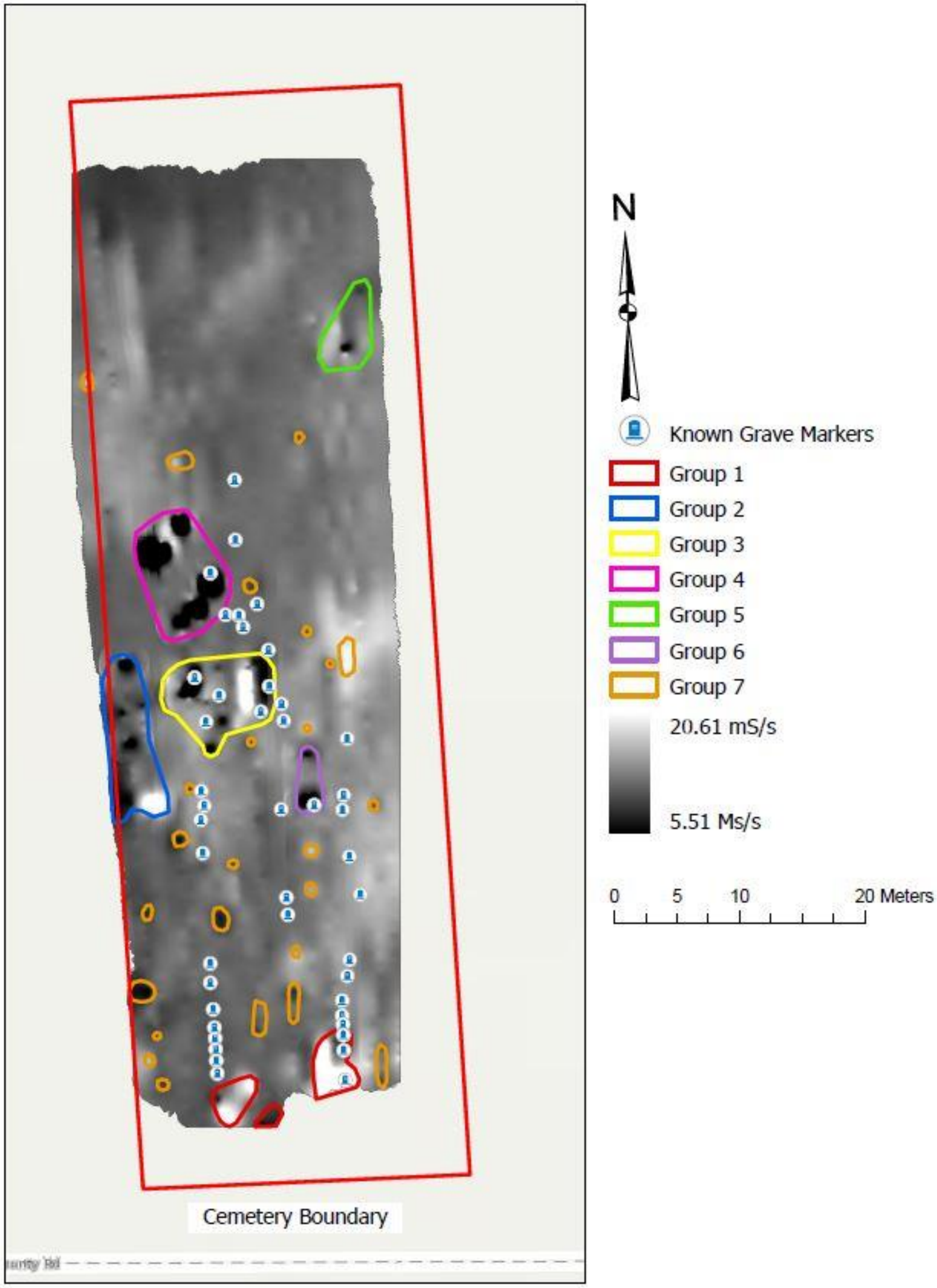

Figure 16: Conductivity data collected during the EMI survey at Evangelical Lutheran Cemetery with anomalies and markers highlighted.

Kingston Cemetery

Geophysical methods deployed at Kingston cemetery included GPR, Magnetometry, and EMI. Both the portions of the cemetery with marked burials and with potential unmarked burials were included in the surveys. This was done to allow comparisons between these two areas to be made within the same data sets. GPR data collection at Kingston Cemetery was done in two grids, the composites that were generated with the radargrams from these grids were separated into four data sets as the samples per a scan were adjusted during the collection of the two grids. This data was collected with help from employees of the EYCCB on August 18, 2021 and August 19, 2021. The resulting four grids include a northwest grid (A) that is 21.5 x 40 m in size, a northeast grid (B) that is 48 x 40 m, a southwest grid (C) that is 35 x 40 m, and a southeast grid (D) that is 35 x 40 m. The radargrams have been used to generate a two-dimensional composite image of the survey at an approximate depth of 1 m, these were than used to identify anomalies. Grid A has eight anomalies that are between 1 and 3 m along their longest axis (Figure 17). Grid B contains six anomalies between 1 and 3 m in length at their largest (Figure 17). Grid C has twelve anomalies ranging from 1 to 3 m along their long axis (Figure 17). Grid D has one anomaly between 1 and 2 m along the western boundary (Figure 17). The anomalies highlighted are caused by extreme reflectors seen in the corresponding radargrams as these are the only reflectors that contrast significantly enough from the background noise on the radargrams. In the radargrams this noise can be seen as multiple weak reflectors that are punctuated with extreme anomalies (Figure 18).

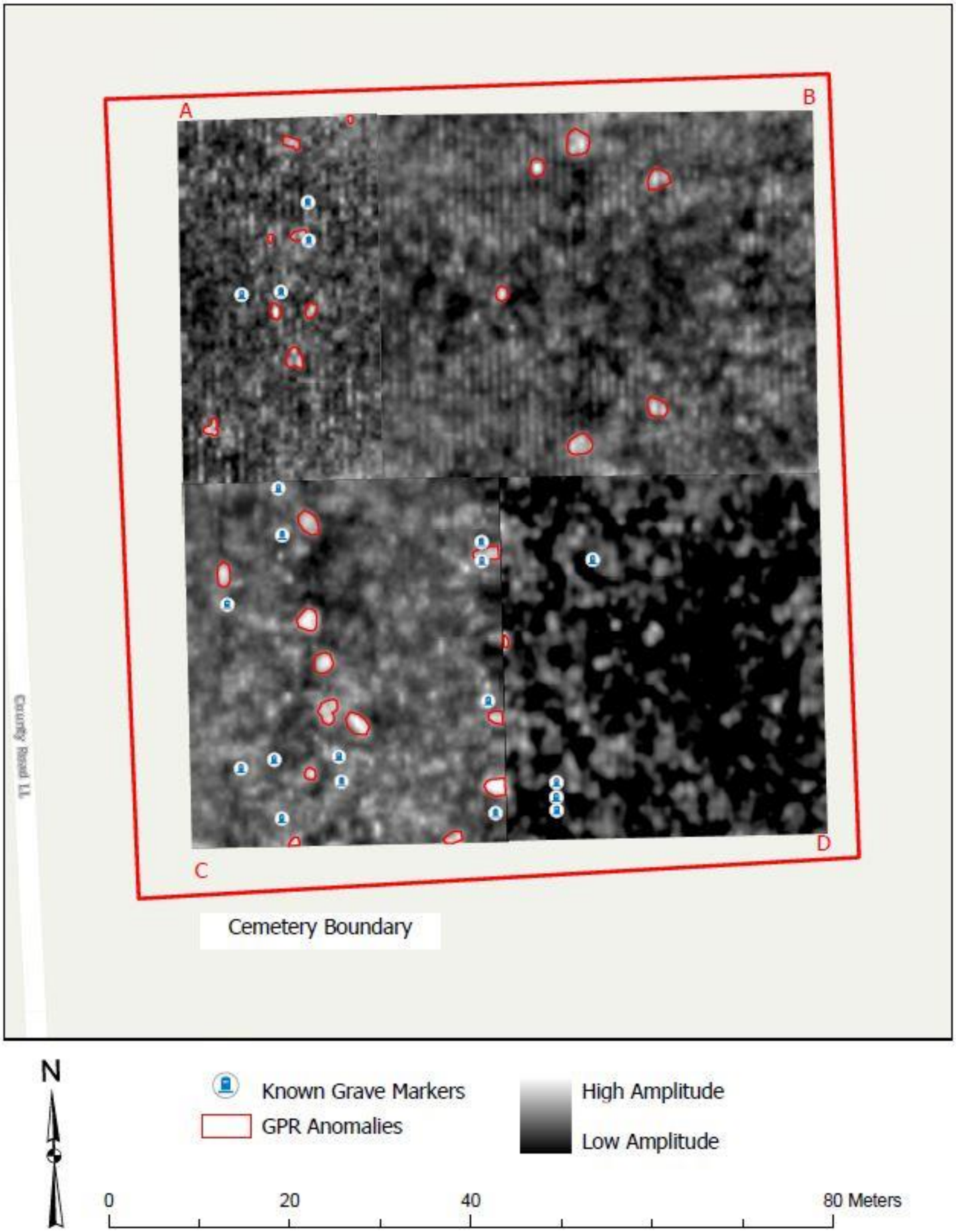

Figure 17: Composite of the four gridded GPR results at Kingston Cemetery with anomalies and markers highlighted.

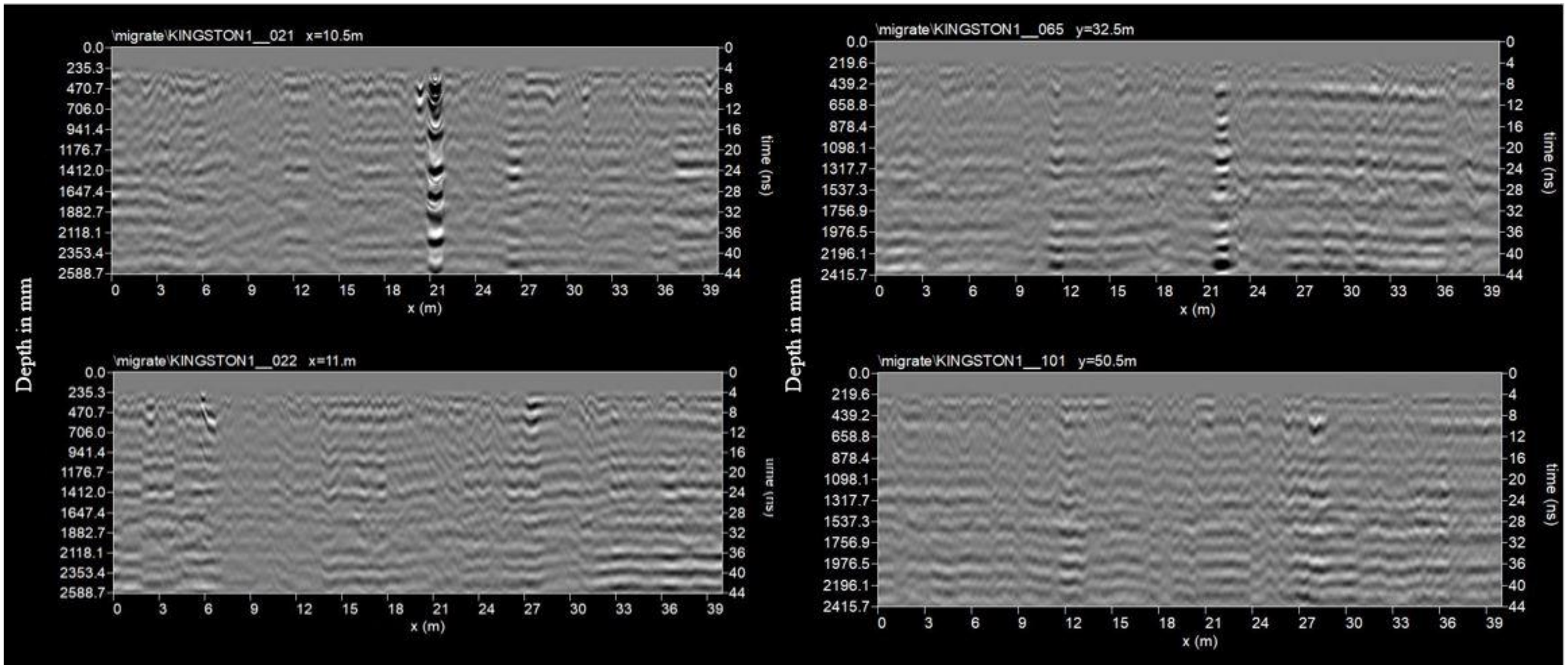

Figure 18: Example of radargrams from Kingston Cemetery, the two on the left are from grid A, the two on the right are from grid B.

Magnetometry data at Kingston Cemetery was collected as one large grid and was processed as such. I collected this data on June 1, 2022. Anomalies at the site were numerous and have been sorted into six groups determined by their relative positions, known sources of disturbance, and intensity (Figure 19). Group one is in the southwest corner of the survey area, centered around 8 m east of the western boundary and 11 m north of the southern boundary (shown in red in Figure 19). The group is linear with the long axis oriented in the north-south direction and extending approximately 20 m, the maximum width is around 11 m. Group two is also located in the southwest, centered 9 m east of group one, though the groups are adjacent (shown in blue in Figure 19). The second group has a linear shape and is slightly smaller than group one, measuring 16 m north to south and 7 m east to west. Group three extends from the southern boundary north at the east-west center of the survey area (shown in green in Figure 19). The center of group three is around 33 m east of the western boundary and 20 m north of the southern boundary. This group is the largest of the six and forms a linear shape with a long axis extending to the north around 38 m having a maximum width of around 17 m. Group four is in the northwest portion of the survey area, centered around 9 m east of the western boundary and 61 m north of the southern boundary (shown in yellow in Figure 19). The L-shaped group is smaller than the previous groups at around 9 m from east to west and 7 m from north to south. Group five includes two linear clusters of anomalies that are on the western and eastern boundaries of the survey area (shown in purple in Figure 19). The western cluster is around 15 m in length and is centered approximately 50 m north of the southern boundary while the eastern cluster extends north from the southeast corner around 52 m. The western cluster is adjacent to the small metal awning covering the cemetery's sign while the eastern cluster is adjacent to the eastern boundary fence. Group six includes the anomalies that are more isolated and do not fall into groupings as easily (shown in pink in Figure 19). These anomalies occur across the entire survey area and include 26 identified anomaly clusters each containing one or two distinct anomalies. There is one portion of the survey area that has only one identified anomaly, centered around 46 m east of the western boundary and 56 m north of the southern boundary. This area is around 25 x 50 m in size and can be seen in the northeast quarter of the survey area, which contains no burial markers.

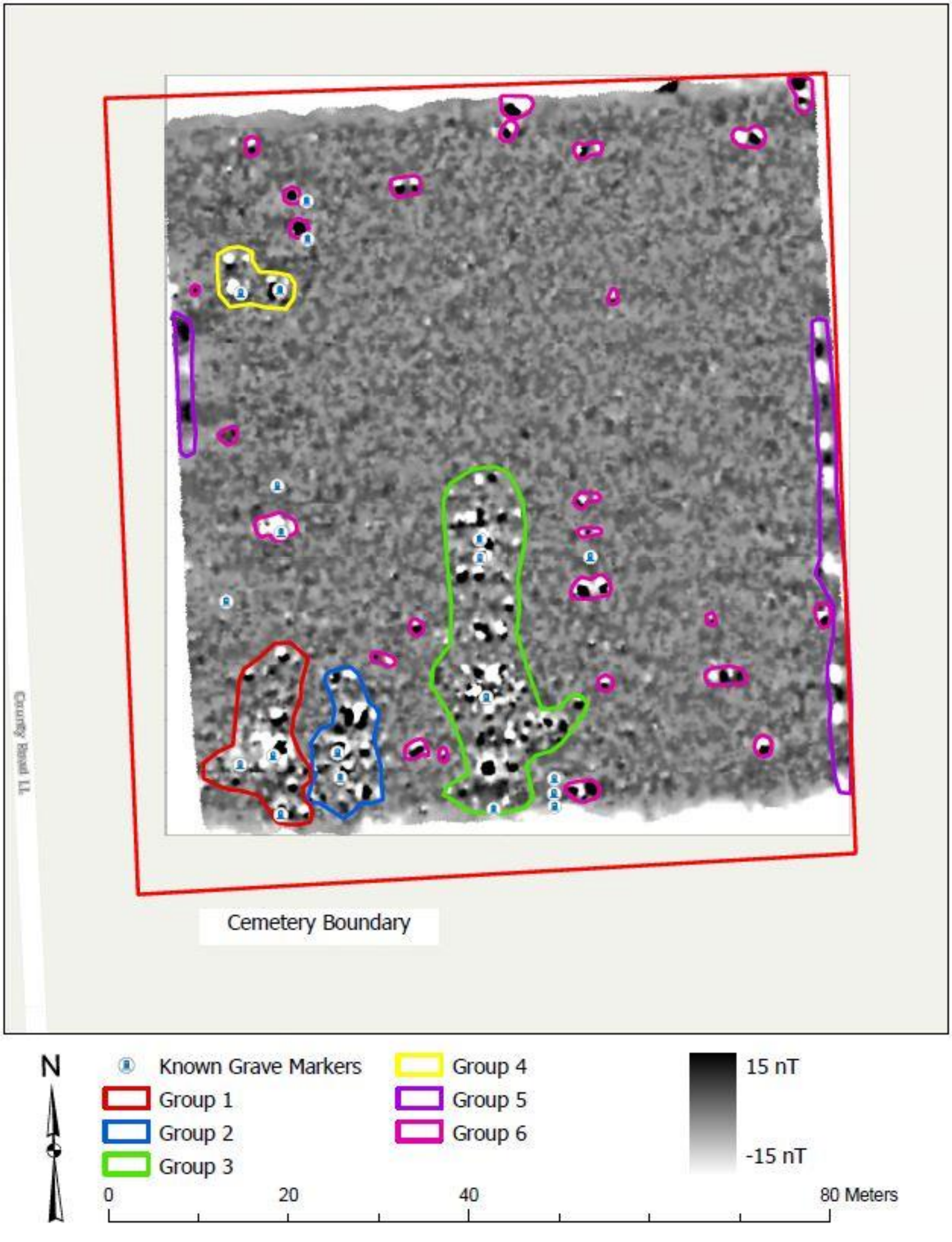

Figure 19:Magnetometry results from Kingston Cemetery with anomalies and markers highlighted.

The two grids of EMI data collected at Kingston Cemetery were processed and gridded together to form a composite. Like at Evangelical Lutheran Cemetery the 50 cm conductive data was the primary set utilized in interpretation, this was again due to recurrent signals in the data sets (Figure 20). This data was collected with help from employees of the EYCCB on March 25, 2022. The anomalies in the conductivity data have been separated into six groups based on their proximity to other anomalies, known sources of disturbance, and intensity (Figure 20). Group one represents the isolated higher intensity anomalies, there are 34 of these anomalies identified within the group that are spread across the survey area (shown in red in Figure 20). The northern half contains four anomalies, three of which are seen in the west and one found in along the eastern boundary. One anomaly is seen straddling the area where the two grids are joined. The other 29 anomalies are in the southern grid. All but three of these southern anomalies are found near the known grave markers in the southwest of the site. The three exceptions are along the eastern boundary of the survey area. Group two represents an anomaly approximately 12 m north of the southern boundary and 25 m east of the western boundary of the survey area, the anomaly is approximately 3 x 5 m in size (shown in blue in Figure 20). Group three is a cluster of anomalies on the western side of the survey area (shown in green in Figure 20). The group of anomalies is centered 40 m north of the southern boundary and 20 m east of the western boundary. The group is slightly linear with a long axis of around 30 m and a width around 20 m. Group four is in the northwest portion of the survey area, centered around 60 m north of the southern boundary and around 10 m east of the western boundary (shown in yellow in Figure 20). The group is linear with a long axis extending around 25 m in the northeast-southwest direction, and a width of approximately 10 m. Group five extends 20 m west from the eastern boundary with around 20 m of extension towards the north (shown in pink in Figure 20). Group six extends along the southern boundary around 55 m from the southeast corner (shown in purple in Figure 20). This group is adjacent to the barbwire fence at the southern boundary of the cemetery.

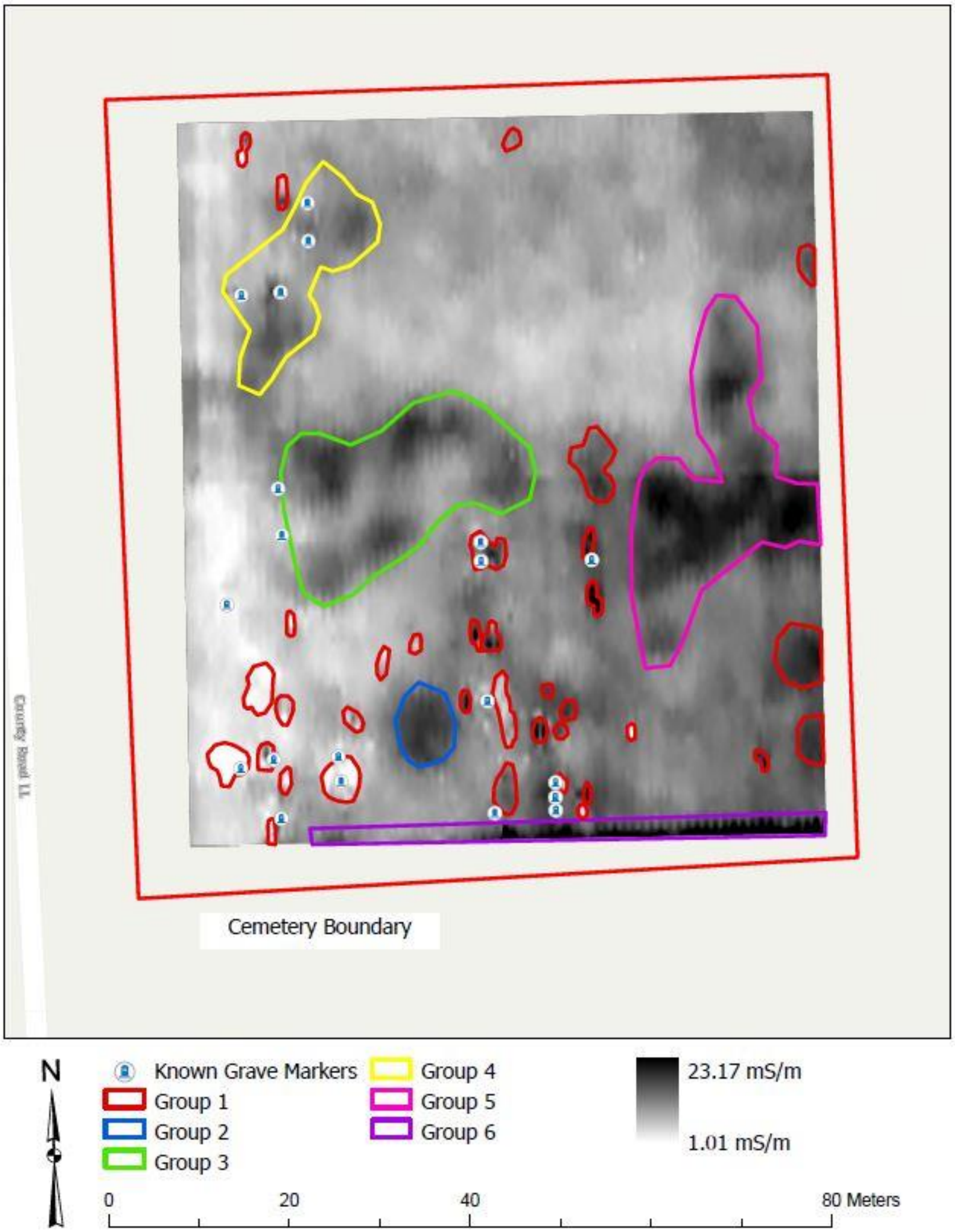

Figure 20: Conductivity data collected during the EMI survey by the sensor spaced 50 cm apart at Kingston Cemetery with anomalies and markers highlighted.

Chapter 5: Discussion

My discussion of the results will be focused on providing the most relevant information to my community partners depending on their goals. I compared the results of the various geophysical techniques utilized at each of the three sites with historical information to identify locations at the respective sites with the potential to contain unmarked burials. The results from the Gould Community Center were inconclusive in identifying the potential for unmarked burials. The interpretation of the data from Evangelical Lutheran Cemetery provided evidence that the northern quarter of the cemetery is unlikely to contain unmarked burials. Finally, the data from Kingston Cemetery has been interpreted to show which parts of the cemetery is least likely to contain unmarked burials, that area being the northeast quarter with an exception along the northern boundary (Figures 27 and 28). I will discuss these interpretations as well as the difficulties in identifying individual graves at these sites and the notable exceptions to the general trends observed.

Gould Community Center

Using GPR and ERT techniques I was not able to locate any anomalies that I could confidently identify as potential burials. However, I was able to correlate large resistive anomaly to the standing marker as well as several smaller reflective anomalies. The complicated history of this site makes confident identification of the sources of geophysical anomalies unfeasible. The anomalies found are as likely to be buried rocks of varying sizes, fragments of building material, or other sorts of debris commonly left behind by the various occupants of the site. Additionally, I determined that the anomalies are more likely to represent buried rocks due to their large size and the layering that was observed in the GPR data (Figures 7, 8, and 9). Crystalline rocks that are common to the river valley are likely to cause high apparent resistivity values and are expected to form large buried clasts in environments like the one observed at the site (Burger et al., 2006). The resistive values match what is to be expected for soils that contain a mix of sand, gravel, and larger fragments in dry conditions which matches the project area during the time of data collection (Burger et al., 2006). The resistive layering of the subsurface and the layering visible in the radargrams suggests there has been little disturbance of the sediment after deposition (Figures 7, 8, and 9). The resistive anomaly between the 4-meter and 6-meter mark visible on G-E-2 corresponds with a high amplitude area on the composite of the GPR grid at a depth slice of around 75 cm (Figure 8). This anomaly cuts through G-G-004 where the anomaly matches the flat stratified layering seen throughout the radargram. The results of this geophysical survey could not be used to confidently identify any of the anomalies within the project area and suggests that the site has experienced relatively few deep disturbances in the stratigraphy at the site. However, it is important to note that geophysical methods are imperfect and can only see buried materials if they are significantly different from the surrounding soil. There are detectable anomalies in the subsurface, it is just beyond the ability of these geophysical methods to confidently identify the sources of these anomalies.

Evangelical Lutheran Cemetery

I combined information from the four geophysical surveys conducted at Evangelical Lutheran Cemetery with the historical data provided by my community partners. Generally, the data shows anomalies are concentrated in the southern three-quarters of the cemetery, near the visible markers. While human activity, and thus likely burials, were visible in the data the presence of individual burials was difficult to reliably identify. Additionally, there are several anomalies that are isolated in the northern portion of the cemetery, these anomalies appear on multiple data sets and represent exceptions to the general trend (Figures 13, 15, 16, and 21).

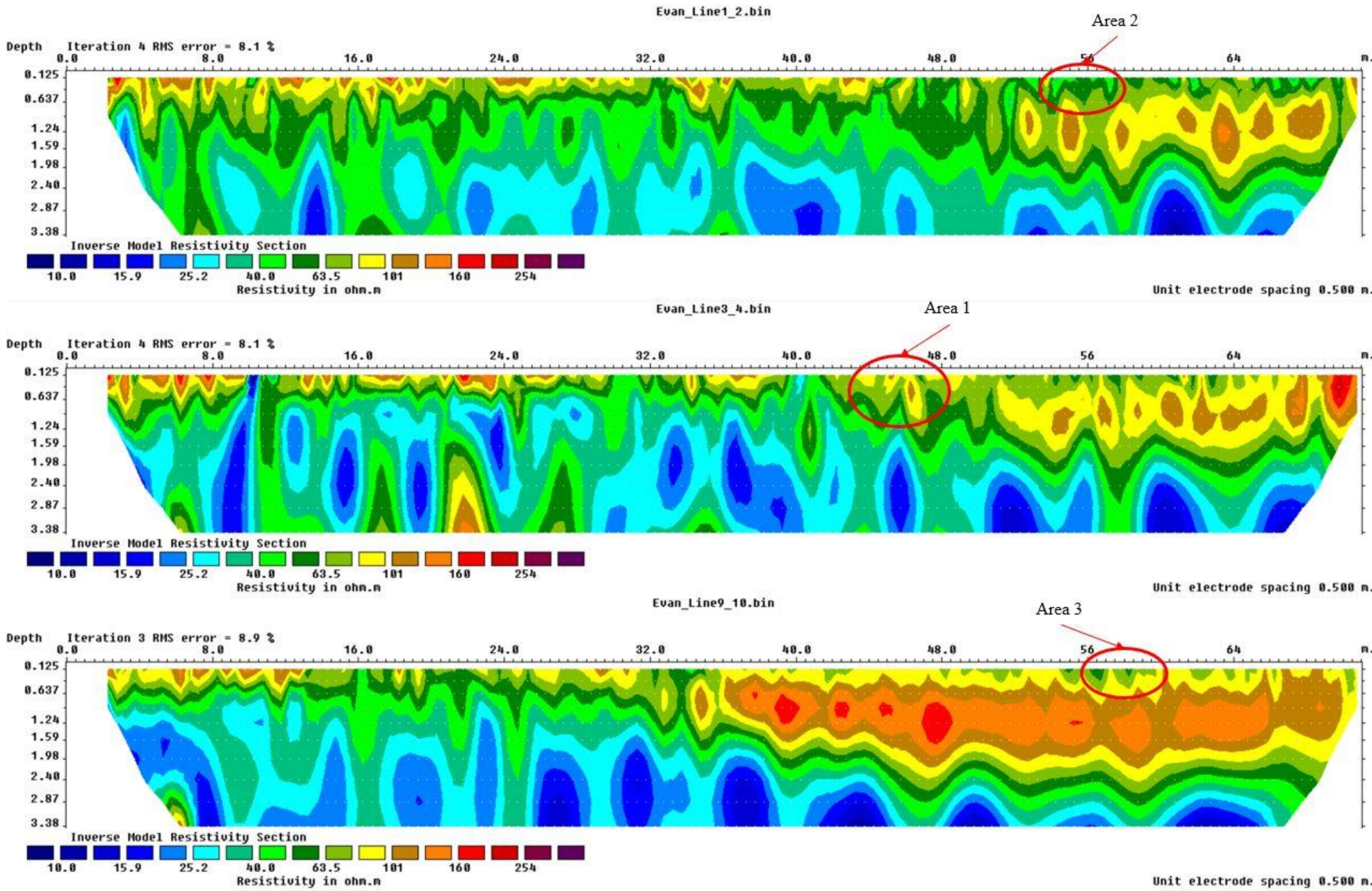

Figure 21: Anomalous areas 1, 2, and 3 at Evangelical Lutheran Cemetery on the resistive models of ERT lines 1 (1_2), 2 (3_4), and 5 (9_10).

In the results section I noted the resistive layering visible in the inversion models of the five ERT lines as well as various small anomalies in that shallow layer. The shallow layer identified in the five lines thickens in the north, it also extends further south in the eastern lines (Figure 12). This matches the presence of the known burial markers which are most abundant in the southwest corner of the cemetery and gradually reduce in number as you move north and east. The increased thickness seen in the layer with higher apparent resistivity correlates with the unmarked parts of the cemetery. I have interpreted this as relating to the level of disturbance the soil has experienced since it was deposited. The smaller anomalies would then likely be related to disturbances of the soil's natural layering, possibly grave shafts. However, the poor resolution of the ERT data makes identifying the boundaries of individual graves difficult. Finally, the areas that have been identified as exceptions to the general trend of the site have been identified in the inversion models of lines one, two, and five (Figure 21). While there are small anomalies visible in the areas highlighted, they are not significantly different from neighboring anomalies to be considered collaborative.

The composite gridded GPR data provides a planer image of the subsurface at an approximate depth of 1 m. This grid shows high amplitude anomalies throughout Evangelical Lutheran Cemetery with noticeable concentrations of anomalies in the south of the cemetery (Figure 13). A significant number of the anomalies seen in the south of the cemetery can be correlated to visible burial markers, this correlation is strongest when the markers are flush with the ground's surface. These flush markers are constructed with reinforced concrete and include small metal plates set in the center of them. An example of the anomalies that correlate with these burial markers can be seen in radargram 003 from the southern grid collected at Evangelical Lutheran Cemetery (Figure 14). Notably the icons representing burial markers in the figures in this thesis are centered on the eastern edges of the markers resulting in the anomalies appearing slightly west of the real-world marker (Figure 13). I have identified no individual burials using GPR at the site. However, I have interpreted the concentration of anomalies in the south as evidence of increased human activity, which in a cemetery setting suggests the possibility of burials. In the northern half of the cemetery there are three high amplitude anomalies that appear unrelated to burial markers and correlate with anomalies present in other data sets. All three anomalies can be seen in the radargrams. However, only two of these anomalies are visible in the 1 m grid slice, the third is visible in a 50 cm grid slice (Figure 22). These anomalies represent the locations of the exceptions to the usual concentration of anomalies in the south of the site.

The magnetometry result from Evangelical Lutheran Cemetery also show a concentration of anomalies in the south of the cemetery. The large magnetic high along the southern boundary is likely caused by the presence of overhead powerlines, which produce electromagnetic fields that dominate other signals (Figure 15). The anomalies in groups two through four are centered around the largest collection of known markers seen in the cemetery. Additionally, at least two anomalies in group eight are associated with known burial markers. Many of the markers in the cemetery contain ferromagnetic metal, which can be seen in the intensity of the anomalies associated with them. For example, the large anomaly that can be seen as the southwest portion of group four is associated with a marker that consists of a steel fence post shaped into a cross (Figure 15). Weaker signals, which possibly relate to disturbed soils, are also found mainly in the southern part of the site reinforcing the conclusion that the majority of the activity at the site occurs there. The large anomalies of groups five, six, and seven occur in areas with no visible metal at the surface. These areas represent exceptions to the southern focus of the anomalies in the data (Figure 15).

Conductivity at Evangelical Lutheran Cemetery shows close associations with the known burial markers and conductive anomalies at the site. Groups one through five are associated with the known markers in the south of the survey area (Figure 16). Additionally, the greater variation in the conductivity in the southern portion of the survey area mirrors the resistivity data suggesting more disturbance to the soil in that area. Individual burials are not visible in the data set as evidenced by the lack of anomalies near known markers. However, groups five and seven contain anomalies that represent exceptions to the southern concentrations and are found in the same locations as the exceptions identified in other data sets.

Combining the ERT, GPR, magnetometry, and conductivity data I collected allows me to draw three insights into the subsurface at Evangelical Lutheran Cemetery. First, individual burials at the cemetery are difficult to define with geophysical methods, but areas with likely burials can be identified. This likely is related to the ages and sizes of the burials. Evangelical Lutheran Cemetery was closed in the early 20th century, with the last marked burial being in 1908. Burials in the rural United States at this time were typically done with burial shrouds or wooden coffins, neither of which preserve well when buried (Laderman, 2003). These kinds of burial containers produce weak signals in geophysical surveys even if they are preserved. The period the cemetery was active is also reflected in the ages of the individuals that were interred there. Most of the burials marked in the cemetery, around 70 percent, are those of individuals that were younger than 10 years of age. This is to be expected given the high infant mortality of the late 19th and early 20th centuries in rural Colorado. Commonly graves were dug to size, resulting in smaller grave shafts that are more difficult to image with geophysical equipment (Laderman, 2003).

Second, the south of the cemetery is where the majority of the burials are located. The geophysical data shows that soil disturbances are concentrated in the south with the known burial markers. The ERT data showed a clear pattern of increased resistivity in the northern parts of the lines (Figure 12). The resistive models show that the portions of the lines with the large resistive anomalies expand further to the south on the lines collected further to the east. This matches the distribution of the burial markers at the site, which are concentrated in the south but extend further north in the west of the cemetery. This pattern is also visible in the GPR data where most of the high amplitude anomalies are seen in the south, both in the gridded data and the individual radargrams (Figures 13 and 22). This is true on both radargrams that include grave markers along their paths and those that do not, suggesting the increase in reflectors is caused by more than the presence of the above ground markers (Figures 13 and 22). The magnetometry survey likewise displays a clear divide between the south and north of the cemetery. The number and intensity of the magnetic anomalies generally decreases in the data as the survey moves north and east (Figure 15). This again matches the distribution of the markers, which is at least partially due to the presence of magnetic materials in the markers. However, disturbed soil commonly causes weaker magnetic anomalies that can be detected and signals like these are also less common in the north and east of the magnetometry survey (Bevan, 2017; Bullion et al., 2022). Finally, the conductivity data collected during the EMI survey provides a fourth data set suggesting the south and west of the cemetery has experienced more soil disturbance. Conductive anomalies are likely the result of changes in the concentration of the groundwater caused by the disturbance of the soil (Bigman, 2012; Moffat, 2015; Sea & Ernenwein, 2021).

Finally, there are anomalies that are exceptions to the southern trend seen in all four surveys, and three of these anomalies appear in all data sets. The presence of these anomalies pushes the boundary of the area in the cemetery that should be treated with enhanced caution further north. The three areas are in the northwest and northeast of the cemetery. Two anomalous areas are in the northwestern part of the survey. Area one is around five meters northwest of the isolated group of burial markers that are the furthest north (Figures 13, 15, and 16). Area two is in the northwest of the survey and is around 10 m further north along the western boundary. Area three is approximately ten meters northeast of the nearest marker, along the eastern boundary of the survey area. The ERT survey lines have small anomalies in these locations, but they also show multiple anomalies nearby that are not collaborated (Figure 21). The areas of interest correlate with high amplitude GPR anomalies which are visible in both the gridded data and the radargrams (Figure 22). Area one and three appear as small high amplitude reflections on the combined gridded data at a depth of 1 m (Figure 13). However, all three areas are visible at the gridded depth slice taken from 50 cm, where they are more prominent (Figure 22). The radargrams that represent these anomalies also show that the reflections start at a depth of 50 cm or less (Figure 22). The magnetometry data provides additional information regarding the possible sources of these anomalous areas. There are large magnetic anomalies in all three of these areas (Figure 15). The anomalies present as magnetic dipoles suggesting they are caused by buried metal (Bevan, 2017). The conductivity data only has anomalies in area one and three (Figure 16). Area one contains two large anomalies that are represented as conductive lows with a smaller accompanying conductive high adjacent to them. Area three is represented as two small anomalies, the southern one has both a conductive high as well as a low, while the northern one is an isolated conductive low (Figure 16).

Radargrams that Intersect with Anomalous Areas in the North of Evangelical Lutheran Cemetery

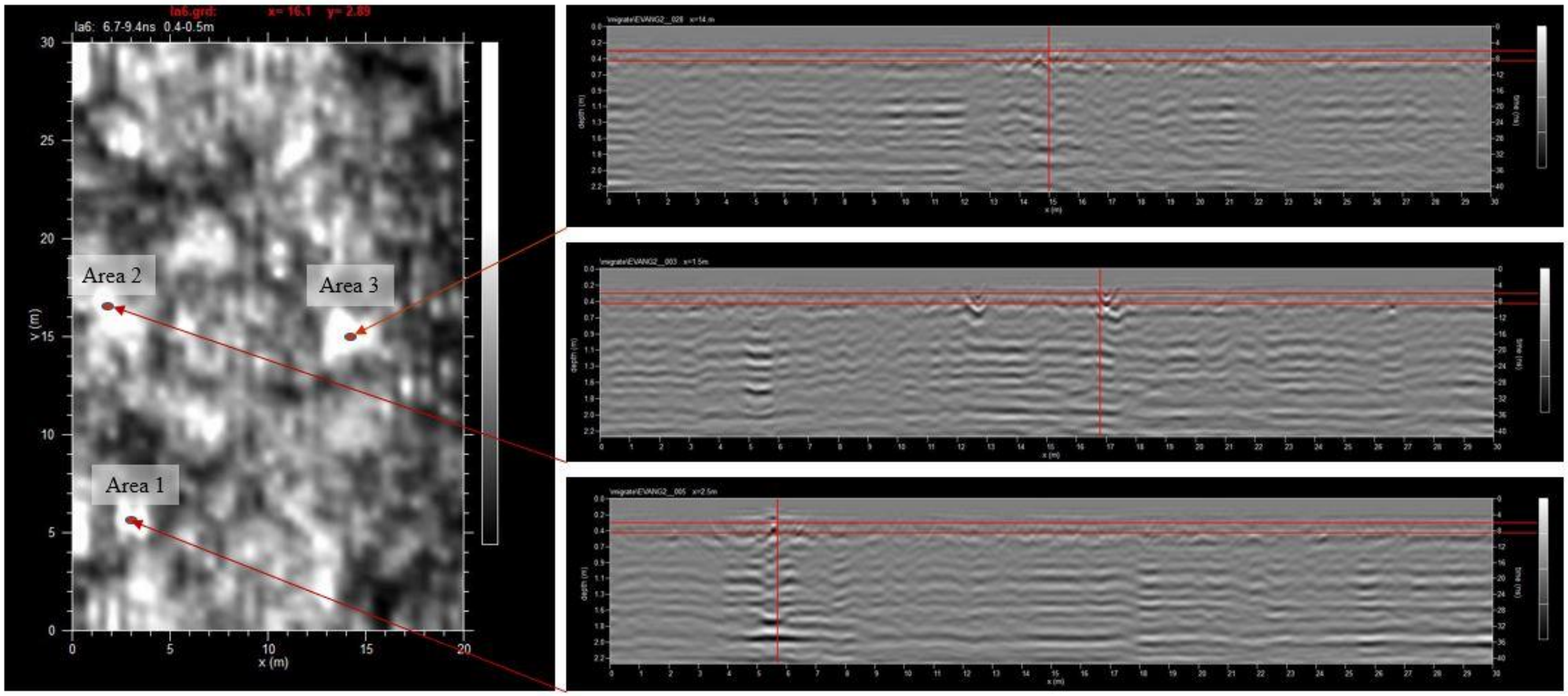

Figure 22: GPR slice of the northern part of Evangelical Lutheran Cemetery with corresponding radargrams.

Kingston Cemetery

I used the historical information provided by my community partners to interpret the combined results from the three geophysical surveys collected at Kingston Cemetery. The resulting understanding of Kingston Cemetery is similar to Evangelical Lutheran Cemetery. This includes the difficulty in identifying individual burials, but the identification of areas likely to contain burials, as well as the identification of exceptions to the general trend observed. At this site the exceptions were also found across data sets but were focused in the magnetometry data (Figures 17, 19, and 20).

I analyzed the GPR survey results as both composite gridded slices of the survey area and as radargrams. The primary focus of this discussion will focus on the depth slice taken from around 1 m (Figure 17). Most of the anomalies I have highlighted are high amplitude reflections which are caused by sharp contrasts in the electrical properties in the ground (Burger et al., 2006; Conyers, 2006). The high amplitude reflections in this survey are only rarely located close to the visible markers at the site, only four of the anomalies highlighted are within 2 m of markers (Figure 17). Many anomalies at the site, both the anomalies near markers and those further away, show large echo shapes in the radargrams (Figure 23). Additionally, the anomalies extend through the entire radargram. This suggests they may be caused by decoupling of the antenna as the echo observed is common when void spaces are encountered and the reflectors begin near the surface (Billinger, 2009). I noted multiple instances of decoupling in my fieldnotes as the cemetery contains open animal burrows and other obstacles that the antenna passed over. The high amplitude anomalies with no echo also commonly start near the surface and appear to extend deep into the ground suggesting strong reflection near the surface by shallow buried materials (Billinger, 2009; Burger et al., 2006; Conyers, 2006). Reflections are common throughout the cemetery suggesting the subsurface is heterogeneous, but this background of multiple reflectors limits the usefulness of GPR in detecting individual burial boundaries. Of note is that the west half of the cemetery was surveyed using a higher samples per scan setting. However, the higher resolution grids do not highlight more anomalies than the lower resolution grids, they simply show a similar number of anomalies at higher resolutions. This can be seen in the side-by-side comparison of radargrams collected 50 cm apart, one at 1024 samples per scan from the east of grid A and the other at 512 samples per scan from the west of grid B (Figure 24). Anomalies are clearly visible in both radargrams, though those collected at a higher resolution are slightly more distinct. The difference evident in the two radargrams does not account for the difference in the number of reflectors visible in the two grids (Figure 17). While these observations in the GPR results demonstrate the limitations of the method at this site general trends can be found. The site has more anomalies located in the west than the east suggesting more disturbance in that part of the site. Additionally, the locations of the anomalies seen in the northeast of the site correlate to other data sets (Figure 17).

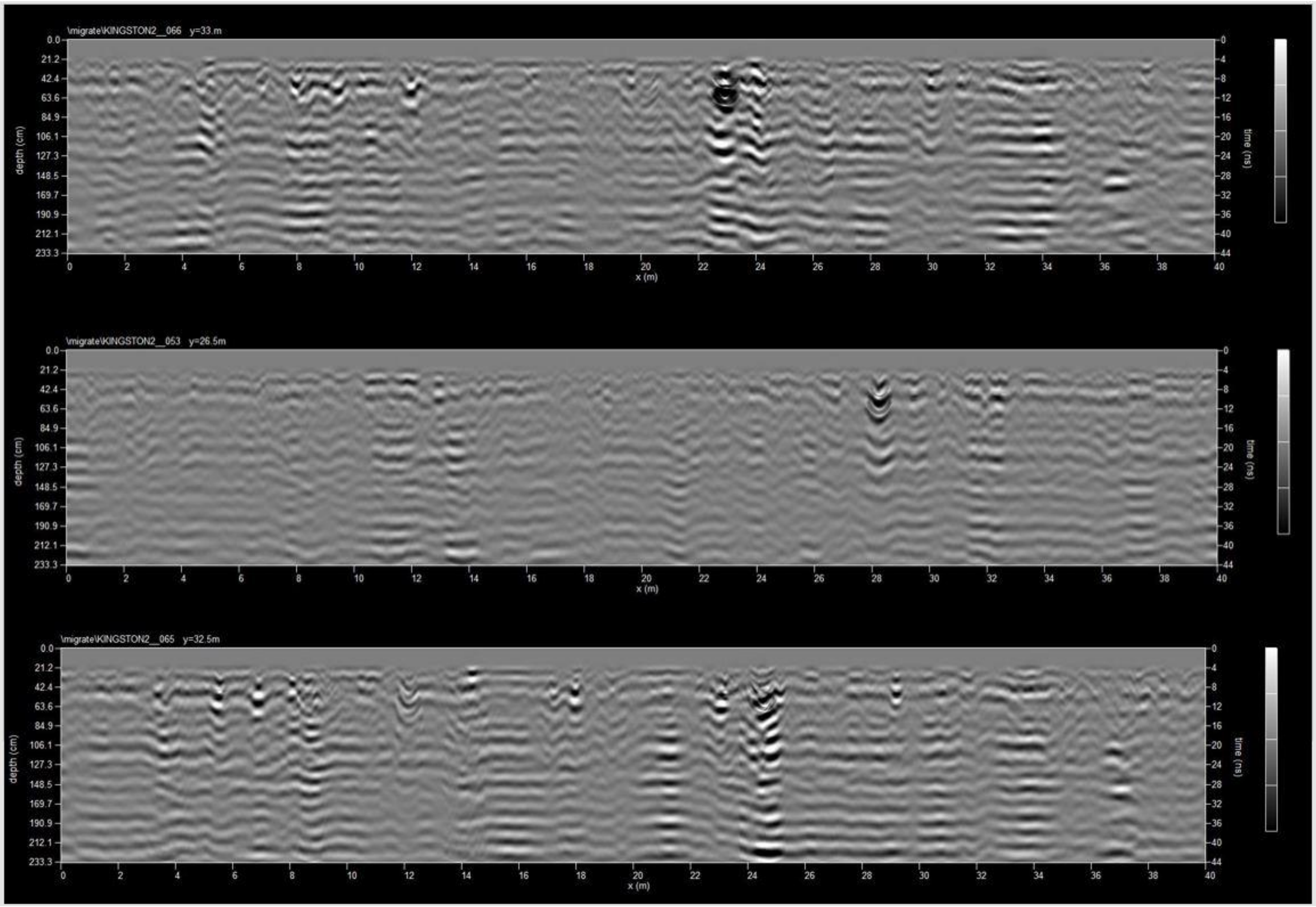

Figure 23: Point-source reflections can be seen likely caused by voids, many of which occur near the surface. Radargrams from grid C of the Kingston Cemetery survey.

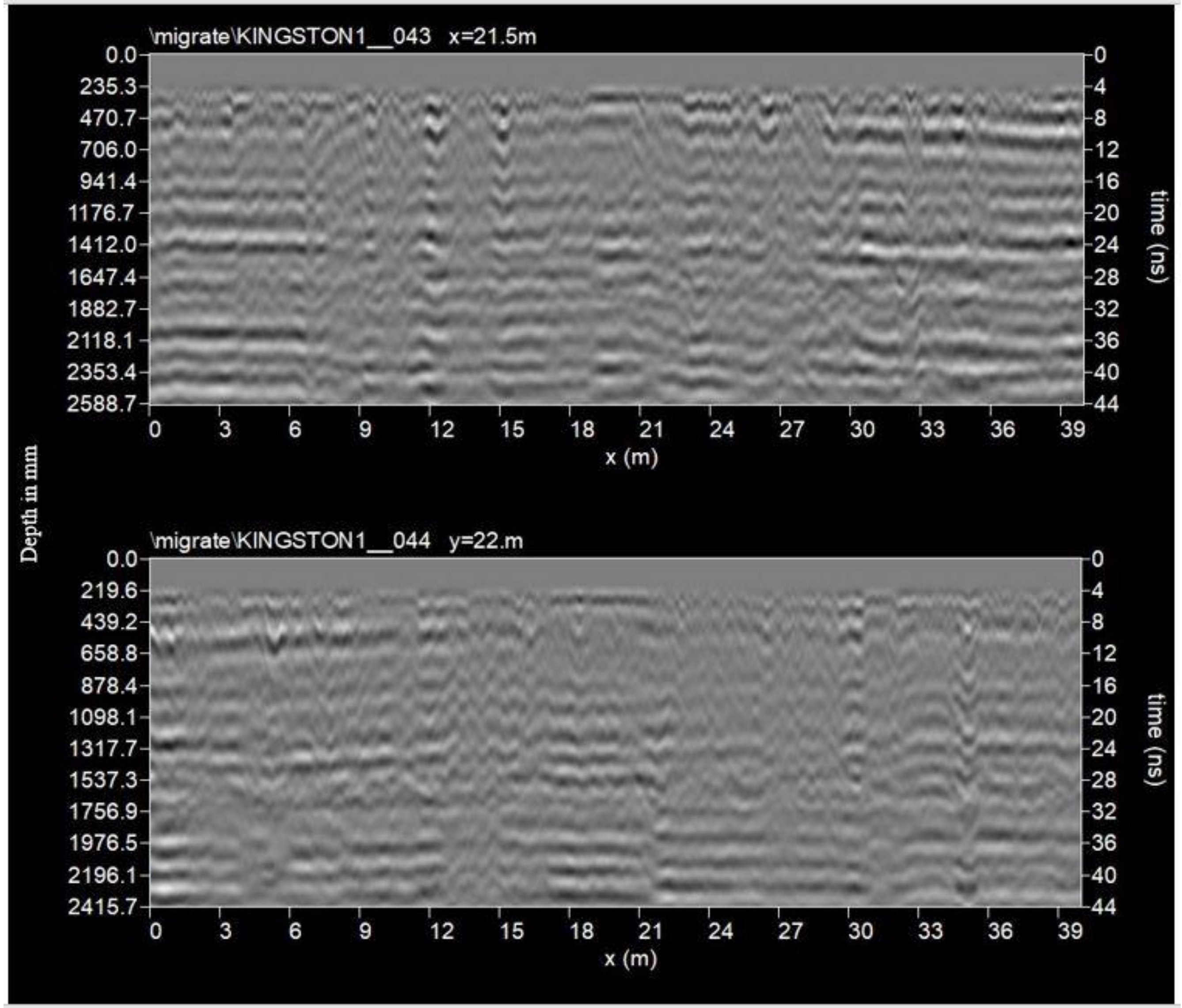

Figure 24: Radargrams from Kingston Cemetery, top is from the east of grid A (northwest grid) and bottom is from the west of grid B (northeast grid).

The results of the magnetometry survey demonstrate a correlation between the visible burial markers at the site and magnetic anomalies (Figure 19). Only two visible markers are not closely related to one or more magnetic anomalies. This can be caused by several factors including the markers themselves, buried mementos left by mourners, possible grave objects, coffin hardware, or soil distributions caused by excavation (Bevan, 2017; Bullion et al., 2022; Burger et al., 2006; Juerges et al., 2010; Springate, 2015). Magnetic anomalies at Kingston Cemetery are predominantly strong dipolar anomalies suggesting they are caused by either easily magnetized objects, such as metal, or objects with their own weak magnetism, such as magnetic minerals (Bevan, 2017). Either of these types of objects are evidence of human activity at this site. Metal is only produced by humans and there are no known geological formations nearby with large quantities of magnetic minerals, but the imported granite or similar stones used as burial markers could contain such minerals (Burger et al., 2006). The use of granite for burial markers at the cemetery can be seen in the standing markers, mostly in the later burials as the material was easier to transport during the later decades of the cemetery's operation. Most magnetic anomalies are found in the south and west of the cemetery, with around six significant exceptions in the northeast part of the site (Figure 25).

Conductivity collected at the site during the EMI survey demonstrates a correlation between the presence of burial markers and conductive anomalies (Figure 20). Only one marker is located more than 2 m from the nearest group of conductive anomalies. The primary factor affecting the conductivity in the cemetery is likely the distribution of ground water (Sea & Ernenwein, 2021). The even distribution seen in the northeast of the site suggests the area has limited disruptions in the soil while the anomaly filled areas near the burial markers demonstrates the opposite (Figure 20). Exceptions to the generally homogeneous northeast can be seen along the northern and eastern boundaries from anomalies in group one as well as the northern extension of the group five anomaly (Figure 20).

Like Evangelical Lutheran Cemetery the combination of the results from the geophysical surveys I collected and the historical information provided by local partners leads to three insights into the subsurface at Kingston Cemetery. First, individual graves at this cemetery are difficult to image using geophysical techniques, but the areas affected by burials can be identified. Most of the known graves are from the late 19th and early 20th century, with only two marked burials occurring after 1920. Additionally, the common occurrence of disproportionately high numbers of sub-adult burials at historical cemeteries is evident at Kingston Cemetery. Around half of the marked burials are of individuals less than ten years of age. The use of burial shrouds or wooden coffins and the smaller average size of burials in cemeteries from this period make burials very similar to the soil surrounding them, particularly after a century of time has passed (Laderman, 2003). Difficulty locating marked burials at Kingston Cemetery is compounded by the tendency of the markers themselves to produce large signals in the geophysical data obscuring the weaker potential responses from the burials. While these factors make locating individual graves difficult at Kingston Cemetery it does not prevent me from using the data to make larger conclusions about the cemetery.

Second, there are parts of the cemetery that have significantly more anomalies than other portions (Figures 17, 19, and 20). In the case of Kingston Cemetery, the northeast quarter of the cemetery is considerably less likely to have geophysical anomalies than the west and south. Unlike the individual burials the larger areas of the cemetery that have experienced soil disturbances can be observed in the data. The concentrations of anomalies in all three data sets are seen in the south and west of the cemetery (Figures 17, 19, and 20). The anomalies are likely related to human activity or animal activity in the form of burrows. I struggled to detect anomalies beyond what appears to be shallowly buried metal or animal burrows at this site when using GPR (Figure 17). However, in the cemetery context both human and animal disturbances typically indicate previously disturbed soil. For human activity this relates to the primary purpose of cemeteries while the animal activity is related to previously disturbed soil being easier to burrow through. Magnetic anomalies have a similar utility in signally possible soil disturbance. Both disturbed soil itself and near surface objects can produce magnetic anomalies (Bevan, 2017; Burger et al., 2006; Juerges et al., 2010). Previously discussed with GPR these sources are likely related to human activity at the cemetery which often occur at or near burials. Conductivity is slightly different in the evidence that it provides as it is largely controlled by the distribution of ground water (Burger et al., 2006; Sea & Ernenwein, 2021). Soil disturbances impact the way water collects in the subsurface making the anomalies more common in areas with disturbed soil. Additionally, buried object can cause anomalies, though these are typically less pronounced than in magnetometry or GPR data (Bigman, 2012; Conyers, 2006; Sea & Ernenwein, 2021).

Finally, there are exceptions to the general trend in the anomalies. The few anomalies that do occur in the northeast of the cemetery are shown to be located primarily along the northern boundary (Figure 25). These anomalies along the northern boundary are at least partially visible in all three data sets, but they are most visible in the magnetometry results (Figures 17, 19, and 20). The anomalies seen in the GPR in this part of the cemetery are largely not collaborated in the other data sets. The exception to this is the north most anomaly seen in grid B of the cemetery, this is where a magnetic anomaly overlaps with the GPR anomaly (Figure 17). The radargram shows this anomaly extends from around 20 cm below the surface to more than 2.5 m and has no hyperbolic shape to it (Figure 26). The magnetometry data suggests that the magnetic source is likely metal as it appears as a dipole in the data (Bevan, 2017). The magnetic anomalies in this portion of the cemetery, including the one collaborated by GPR, also show an interesting tendency to have two dipole anomalies occur adjacent to one another (circled in Figure 25). This dual pattern is of interest due to the concentration of metal hardware on older wooden coffins being found around the head and feet (Springate, 2015). This tendency would result in magnetic anomalies at the head and feet of burials containing wooden coffins with metal hardware used in their construction. The dual anomalies of interest are spaced around 1.5-2 m apart which matches the average height of an adult and are oriented in the east-west direction (circled in red in Figure 25). There are three anomalies that match this pattern in the northeast quarter of the cemetery. Included in these three anomalies is the one that overlaps the GPR anomaly (designated with a red star in Figure 25). The only conductive anomaly in this part of the cemetery is on the cemetery's northern boundary and matches to a large dual magnetic anomaly oriented toward the northeast with a spacing of around 2.5 m (designated with a yellow star in Figure 25). While I cannot determine that the three dual magnetic anomalies are unmarked burials using magnetometry data alone, I would recommend that the areas near them be avoided if the cemetery is reopened.

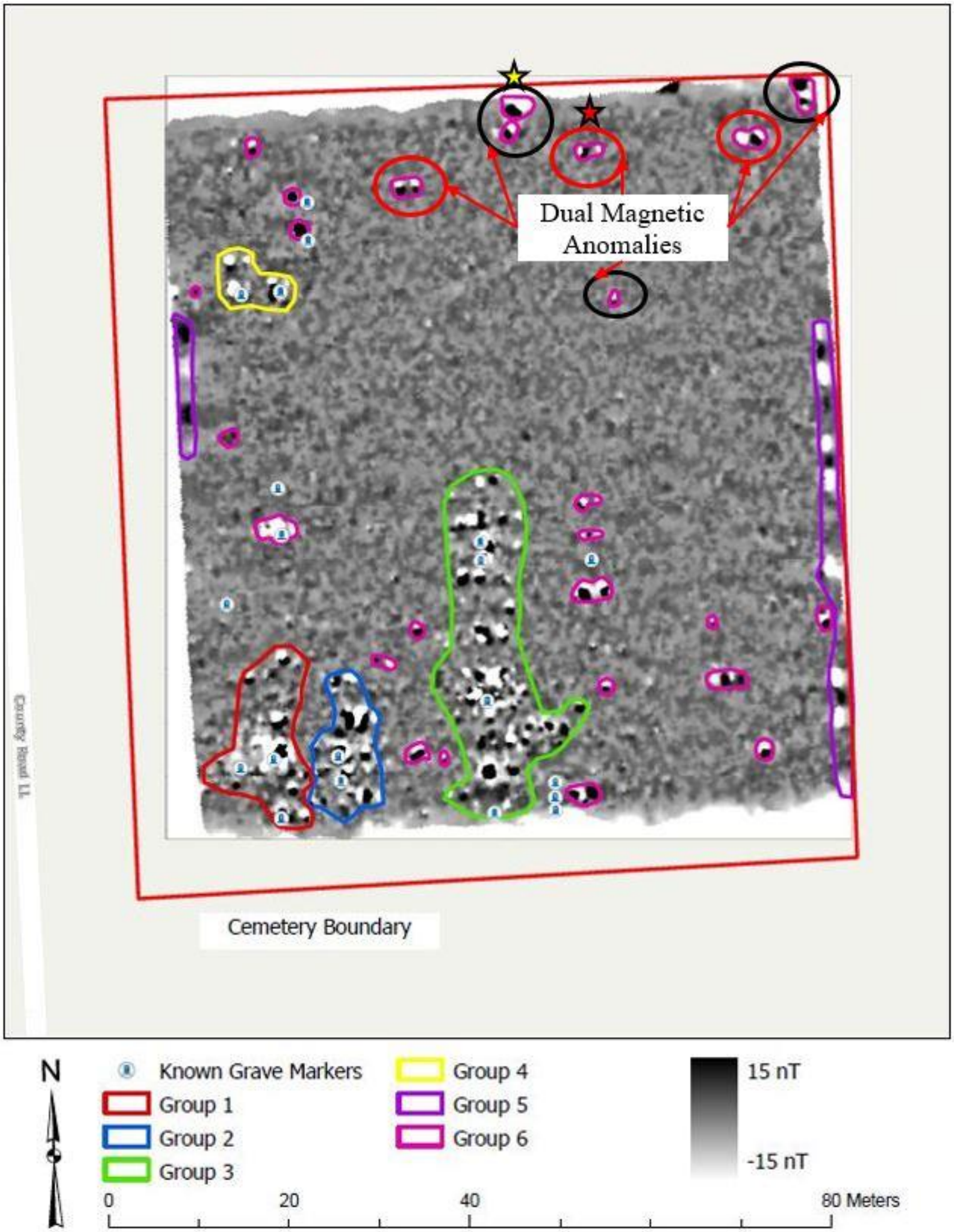

Figure 25: Magnetometry results from Kingston Cemetery with dual anomalies in the northeast circled, in red are possible coffins, the red star marked anomaly matches a GPR anomaly, yellow star marked anomaly matches a conductive anomaly.

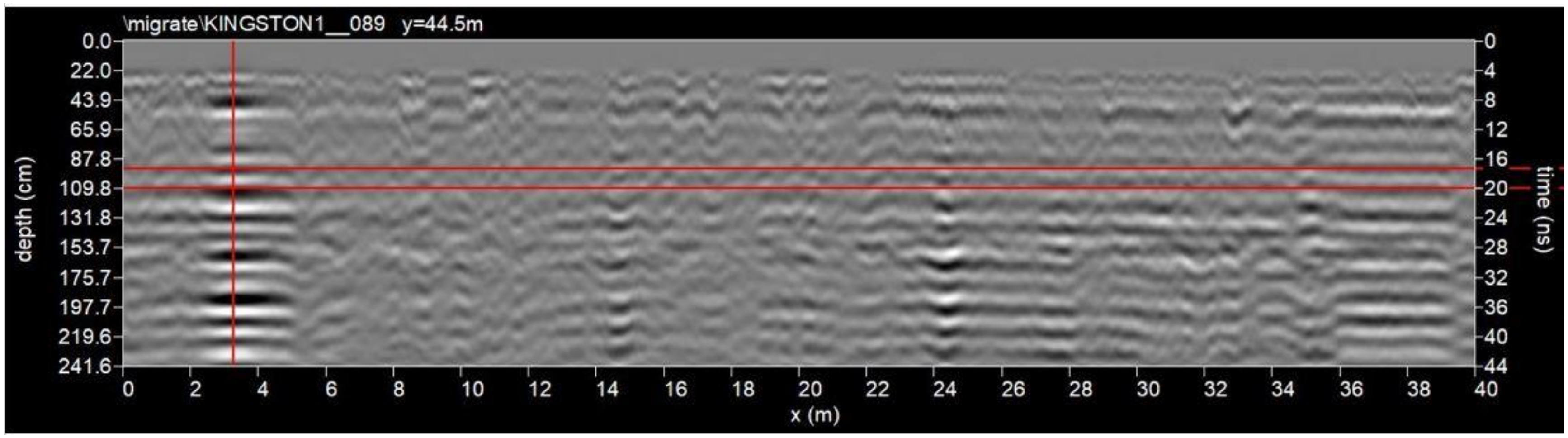

Figure 26: Radargram of the anomaly in grid B of Kingston Cemetery that matches the magnetic anomaly in the same area.

Chapter 6: Conclusion

Historic sites in rural Colorado often have incomplete records on the uses of their land. This can present obstacles to rural communities that are often left to care for these sites and tasked with utilizing the land containing them. As many of these locations were abandoned as populations shifted and settled during the 20th century, they are facing renewed interest in their spaces as the population of Colorado has increased in recent years. This is the case with the communities of Gould and Wray. The small mountain community of Gould uses the site of the former WWII POW camp as their community center, hosting several events at the site for community members and out of town organizations every year. This use of the land causes the community and visitors to spend time at the site on a regular basis. While there they encounter the history of the area and are left with questions regarding the objects that were left behind. These objects include concrete markers that are shaped like stele, a shape often seen in burial markers, which has left the community with concerns about potential unmarked burials at their community center. Community members in Wray, the county seat of Yuma County had similar concerns over two of their own public spaces. Kingston and Evangelical Lutheran Cemeteries were abandoned in the early and mid-20th century as the population of the county declined. These cemeteries came into the care of the EYCCB who now manages the land and is responsible for the preservation of the burials on behalf of the community. Evangelical Lutheran Cemetery is not under consideration for future use, but knowledge of the extent of the area containing burials is useful for the management and preservation of the site. While the extent of the burials at the site is unknown the cemetery retains its historical boundaries which are demarcated by trees and property lines. The knowledge of where inside these boundaries the burials are located however, has been lost. The locations of the burials in Kingston Cemetery are also of interest as the cemetery district is not only concerned with preservation but has also received interest from the broader community in reopening the cemetery to new burials. As a result, the locations of burials are desired so that they can be avoided if new burials are added to the site.

Members of these communities reached out to the CRAG lab at Colorado State University. From this interaction I learned of the sites and visited the community members to discuss their interests. The communities' desires to locate burials at their respective sites made non-invasive archaeological methods ideal, which aligned with my research interests in geophysical methods in archaeology. This led me to offer to perform geophysical surveys of the Gould Community Center, Evangelical Lutheran Cemetery, and Kingston Cemetery for my master's thesis with the understanding that I would share my results with the respective communities. As a result, all findings will be sent to the community members after the completion of this thesis.

I combined geophysical techniques with the historical knowledge collected by the community members in my thesis. Combining this knowledge allowed me to gain insights into the subsurface of the three sites. At the Gould Community Center, I utilized ERT and GPR to survey a small, wooded area on the boundary of the old POW camp that contained several concrete markers. The forest obstruction limited the use of geophysical instruments, however the data collected showed the subsurface at the site contains several anomalies ranging from 50 cm up to several meters in size. Many of these anomalies are likely caused by the large clasts common in the near surface geology of mountain valleys, like the one containing the site. This data combined with the knowledge that the site has had multiple uses in its history, led to my conclusion that geophysical techniques cannot be relied on to confidently identify the causes of anomalies in the subsurface. While anomalies can be imaged at the site, I could not reliably identify them or assume any connection to potential burials.

At the two cemetery sites in Yuma County the issue of numerous land uses is controlled as the cemeteries have only been used for this purpose since the land was occupied by American settlers in the late 19th century. Additionally, the near surface geology in this part of Colorado is dominated by loess with few large naturally occurring disturbances in the soil column. In interpreting the geophysical data collected at the cemeteries I considered both natural and human sources for anomalies observed. Animal burrows were the primary source of non-human disturbance observed in the cemetery. Burrows were noted during data collection and did correlate to a few anomalies in the GPR data. However, the burrows were largely concentrated near the marked burials and did not appear correlate with anomalies in other data sets. This allowed me to confidently assign disturbances collocated in multiple data sets as evidence of human activity, likely associated with burials. While I was unable to identify individual graves, I was able to demarcate areas that are likely to contain burials. At Evangelical Lutheran Cemetery this allows me to identify the southern three-quarters of the cemetery as the portion that is most likely to contain graves, with a tendency to extend further to the north on the western side. Additionally, the cemetery has at least three anomalous areas in the north, where there are fewer anomalies in all available data sets. In interpreting the results, I have concluded that the area of least concern for encountering unmarked burials is the far north of the cemetery. Additionally, I have designated an area along the eastern boundary of the cemetery as an area of moderate concern as there are only small anomalies in the magnetic and conductivity results indicating possible disturbance (Figure 27).

I concluded that Kingston Cemetery has burials concentrated in the south and west of the site. This area also has the most intense concentration of anomalies leading to its designation as the area of highest concern for encountering unmarked burials (Figure 28). The large area in the northeast quarter of the cemetery has few anomalies in the geophysical results. However, along the northern boundary, in the eastern part of the cemetery, there are six magnetic anomalies of interest including one that is collaborated by GPR and another by conductivity. Of these anomalies three are reminiscent of magnetic anomalies caused by wooden coffins, I have labeled them dual magnetic anomalies. While the other three are likely caused by buried metal, they are either oriented in the wrong direction or of the wrong size to be likely burials. Of the three that match possible burials, only one anomaly is collaborated by GPR. The conductive anomaly matches an anomaly that is larger and oriented in an unusual direction. This led to my conclusion that while the northeast is an area of least concern there is a portion along the northern fence line that should be seen as a second area of highest concern (Figure 28). I assigned an area of moderate concern at Kingston Cemetery between the areas of least and highest concern due to the presence of conductive anomalies in that part of the cemetery. These anomalies are not reminiscent of burials and are not collaborated by other results but out of caution were highlighted (Figure 28).

Figure 27: Areas of concern determined by the concentration of anomalies found in the geophysical results at Evangelical Lutheran Cemetery.

Figure 28: Areas of concern determined by the concentration of anomalies found in the geophysical results at Kingston Cemetery.

References Cited

Abbott, C., Leonard, S. J., & Noel, T. J. (2013a). “Exterminate Them!”: Natives 1850s–90s. In *Colorado: A History of the Centennial State* (pp. 81–95). University Press of Colorado. https://doi.org/10.5876/9781607322276:c06

Abbott, C., Leonard, S. J., & Noel, T. J. (2013b). Farming and Ranching in the American Desert. In *Colorado: A History of the Centennial State* (pp. 161–182). University Press of Colorado. https://doi.org/10.5876/9781607322276:c10

Bevan, B. W. (2017). Analysis of dipolar magnetic anomalies. *Technical Report (Geosight)*. https://doi.org/10.13140/RG.2.2.35995.05929/1

Bigman, D. P. (2012). The use of electromagnetic induction in locating graves and mapping cemeteries: An Example from native North America. *Archaeological Prospection*, *19*(1), 31–39. https://doi.org/10.1002/arp.1416

Billinger, M. S. (2009). Utilizing ground penetrating radar for the location of a potential human burial under concrete. *Journal of the Canadian Society of Forensic Science*, *42*(3), 200–209. https://doi.org/10.1080/00085030.2009.10757607

Bradley, E. B. (2005). *Timber Times and Tales, An Early History of Gould, Colorado*.

Bullion, E., Maksudov, F., Henry, E. R., Merkle, A., & Frachetti, M. (2022). Community practice and religion at an Early Islamic cemetery in highland Central Asia. *Antiquity*, *96*(387), 628–645. https://doi.org/10.15184/aqy.2021.106

Burger, H. R., Sheehan, A. F., Jones, C. H., & Burger, H. R. (2006). *Introduction to applied geophysics: Exploring the shallow subsurface* (Vol. 550). WW Norton New York.

Conyers, L. B. (2006). Ground-penetrating radar techniques to discover and map historic graves. *Historical Archaeology*, *40*(3), 64–73.

Doro, K. O., Emmanuel, E. D., Adebayo, M. B., Bank, C. G., Wescott, D. J., & Mickleburgh, H. L. (2022). Time-Lapse Electrical Resistivity Tomography Imaging of Buried Human Remains in Simulated Mass and Individual Graves. *Frontiers in Environmental Science*, *10*. https://doi.org/10.3389/fenvs.2022.882496

Goodman, D., & Piro, S. (2013). *GPR remote sensing in archaeology* (Vol. 9). Springer.

Gray, O. W. (1886). Colorado. In *The National Atlas*. Stedman and Brown.

Haigler. (1885, February 14). *The Brush Lariat*, 1–1.

Henry, E. R., Laracuente, N. R., Case, J. S., & Johnson, J. K. (2014). Incorporating Multistaged Geophysical Data into Regional-scale Models: A Case Study from an Adena Burial Mound in Central Kentucky. *Archaeological Prospection*, *21*(1), 15–26. https://doi.org/10.1002/arp.1474

Homm, B. R. (1999). *Our Pioneer Heritage*. Self-Published.

Johnson, W. J. (n.d.). *Geophysical Detection of Graves 2014 Cemetery surveys for Alexandria Archaeology View project*. https://www.xinxii.com/gratis/122101rd1350746731.pdf.

Juerges, A., Pringle, J. K., Jervis, J. R., & Masters, P. (2010). Comparisons of magnetic and electrical resistivity surveys over simulated clandestine graves in contrasting burial environments. *Near Surface Geophysics*, *8*(6), 529–539. https://doi.org/10.3997/1873-0604.2010042

Laderman, G. (2003). *Rest in peace: A cultural history of death and the funeral home in twentieth-century America*. Oxford University Press, USA.

Lemke, A. (2020). “Missing Cemeteries” and Structural Racism: Historical Maps and Endangered African/African American and Hispanic Mortuary Customs in Texas. *Historical Archaeology*, *54*(3), 605–623. https://doi.org/10.1007/s41636-020-00258-0

Madole, R. F. (1991). Surficial Geologic Map of the Walden 30’ x 60’ Quadrangle, Jackson, Larimer, and Routt Counties, Colorado. In *Department of the Interior U.S. Geological Survey*. Department of the Interior.

Miller, D. M. S., & Rivera, J. D. (2006). Hallowed ground, place, and culture: The cemetery and the creation of place. In *Space and Culture* (Vol. 9, Issue 4, pp. 334–350). https://doi.org/10.1177/1206331206292450

Moffat, I. (2015). Locating graves with geophysics. *Best Practices of Geoinformatic Technologies for the Mapping of Archaeolandscapes*, 45–53.

Muhs, D. R., Bettis III, E. A., Aleinikoff, J. N., McGeehin, J. P., Beann, J., Skipp, G., Marshall, B. D., Roberts, H. M., Johnson, W. C., & Benton, R. (2008). Origin and paleoclimatic significance of late Quaternary loess in Nebraska: evidence from stratigraphy, chronology, sedimentology, and geochemistry. *Geological Society of America Bulletin*, *120*(11–12), 1378–1407.

Rojo Rodriguez, S., & Mckenzie, C. M. M. (n.d.). *The Hernández Family Cemetery (41BX542) and Investigations of the Jesus Hernández (41BX2222) and*.

Rugg, J. (2000). *De® ning the place of burial: what makes a cemetery a cemetery?* (Vol. 5, Issue 3).

Sanger, M. C., Cavanagh, K., Shamoon-Pour, M., Thomas, R., Piekut, L., Bourcy, S., & Seeber, K. (2020). Public archaeology at Baynard-Zion: bringing life back to an antebellum cemetery. *Southeastern Archaeology*, 183–197. https://doi.org/10.1080/0734578X.2020.1786655

Sea, C. D., & Ernenwein, E. G. (2021). Frequency domain electromagnetic induction: an efficient method for investigating Fort Ancient village dynamics. *Archaeological Prospection*, *28*(1), 73–87. https://doi.org/10.1002/arp.1798

Springate, M. E. (2015). *Coffin Hardware in Nineteenth-century America* (1st ed.). Routledge.

Stanger, R., & Roe, D. (2007). Geophysical surveys at the West End Cemetery, Townsville: An application of three techniques. In *Australian Archaeology* (Vol. 65, pp. 44–50). Australian Archaeological Association Inc. https://doi.org/10.1080/03122417.2007.11681858

Sudradjat, I. (2012). Foucault, the Other Spaces, and Human Behavior. *Procedia - Social and Behavioral Sciences*, *36*, 28–34. https://doi.org/10.1016/j.sbspro.2012.03.004

Thompson, V. D., DePratter, C. B., Lulewicz, J., Lulewicz, I. H., Roberts Thompson, A. D., Cramb, J., Ritchison, B. T., & Colvin, M. H. (2018). The archaeology and remote sensing of Santa Elena's four millennia of occupation. *Remote Sensing*, *10*(2). https://doi.org/10.3390/rs10020248

U.S. Department of Veterans Affairs. (2023). *World War II POWs-one (1) Italian and eight (8) German 1. Behrens, Willi, Site 201 2. Fisher, Hans, Site 207 3. Gall, Ernst, Site 199 4. Hafer, Karl Heinz, Site 209 5. Knoph, Heinz Ober, Site 204 6. Camp Butler; three (3) at Camp McCoy, WI; eleven (11) at Fort Robinson, NE; nineteen (19) at Camp Atterbury* (Issue 1). POW.

Vidler, A., Foucault, M., & Johnston, P. (2014). *Heterotopias* (Issue 69).

War Department vs. Michigan River Timber Company. (1944). *Contract for Prisoner of War Labor*.

Worrall, J. E. (1990). Prisoners on the Home Front, Community Reactions to German and Italian POWs in Northern Colorado, 1943-1946. *Colorado Heritage*.

Appendices

Gould Community Center

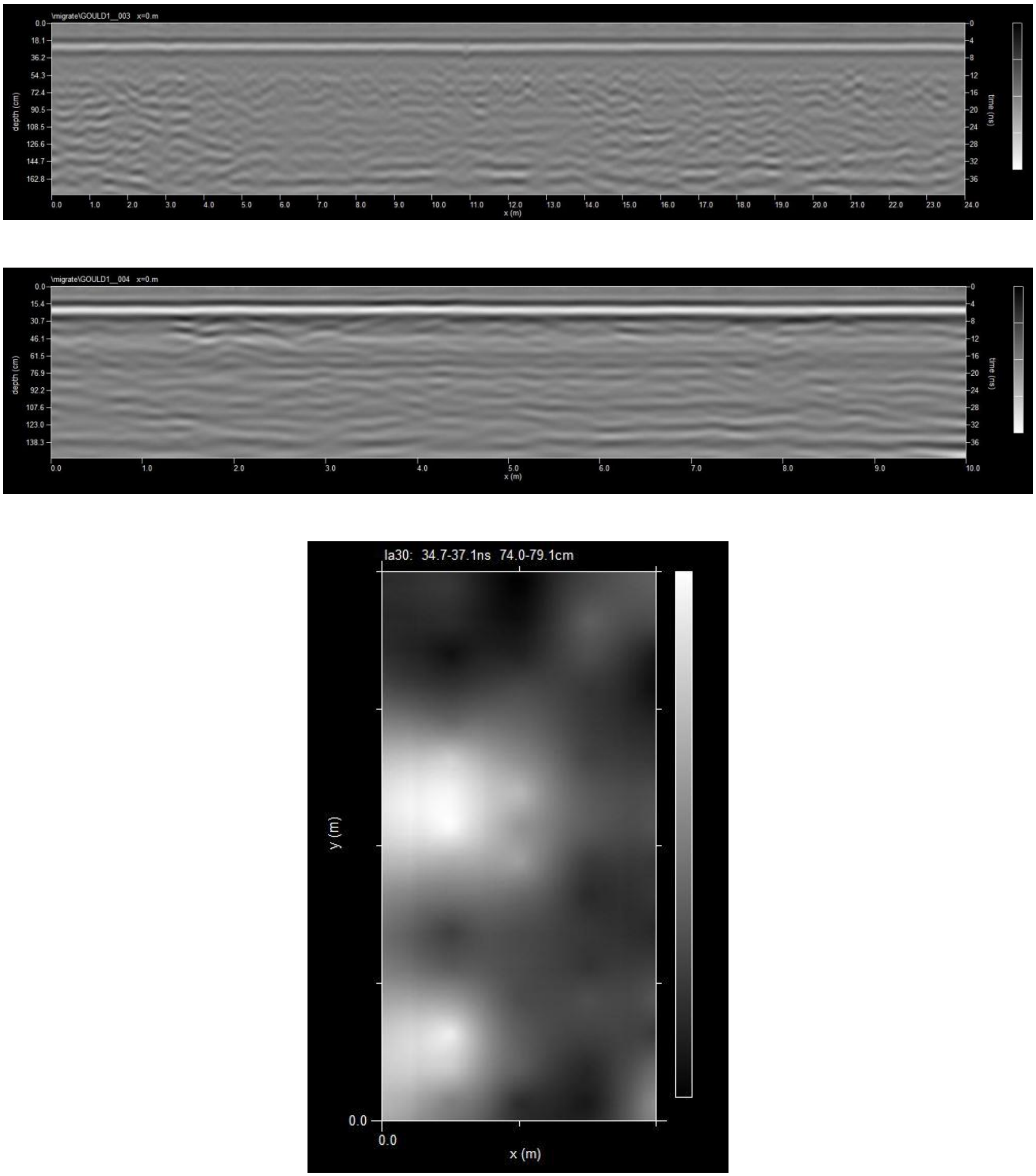

Figure 29: Uninterpreted GPR results from Gould Community Center. (Top, G-G-003), (Middle, G-G-004), (Bottom, G-G-Grid1)

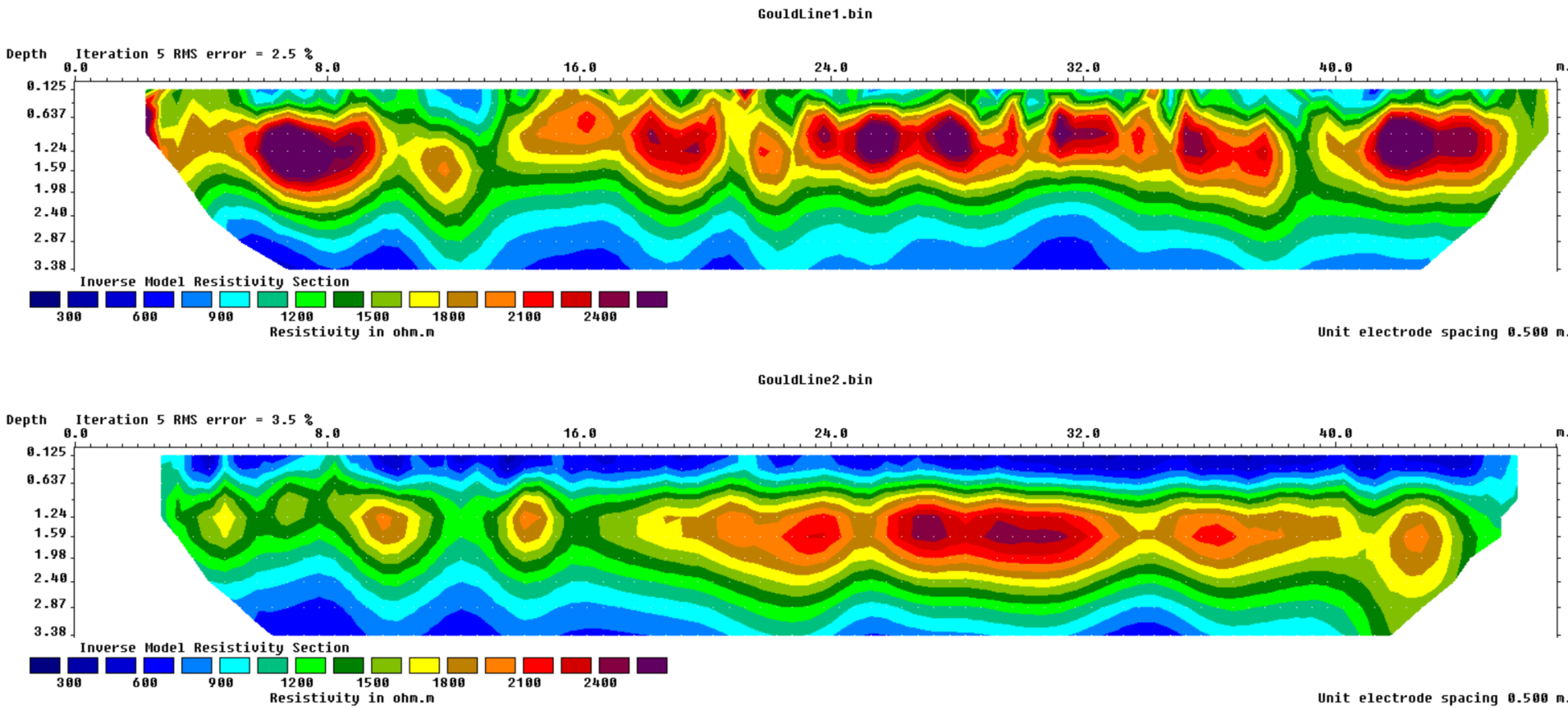

Figure 30: Uninterpreted ERT results from Gould Community Center. (Top, G-E-1), (Bottom, G-E-2)

Evangelical Lutheran Cemetery

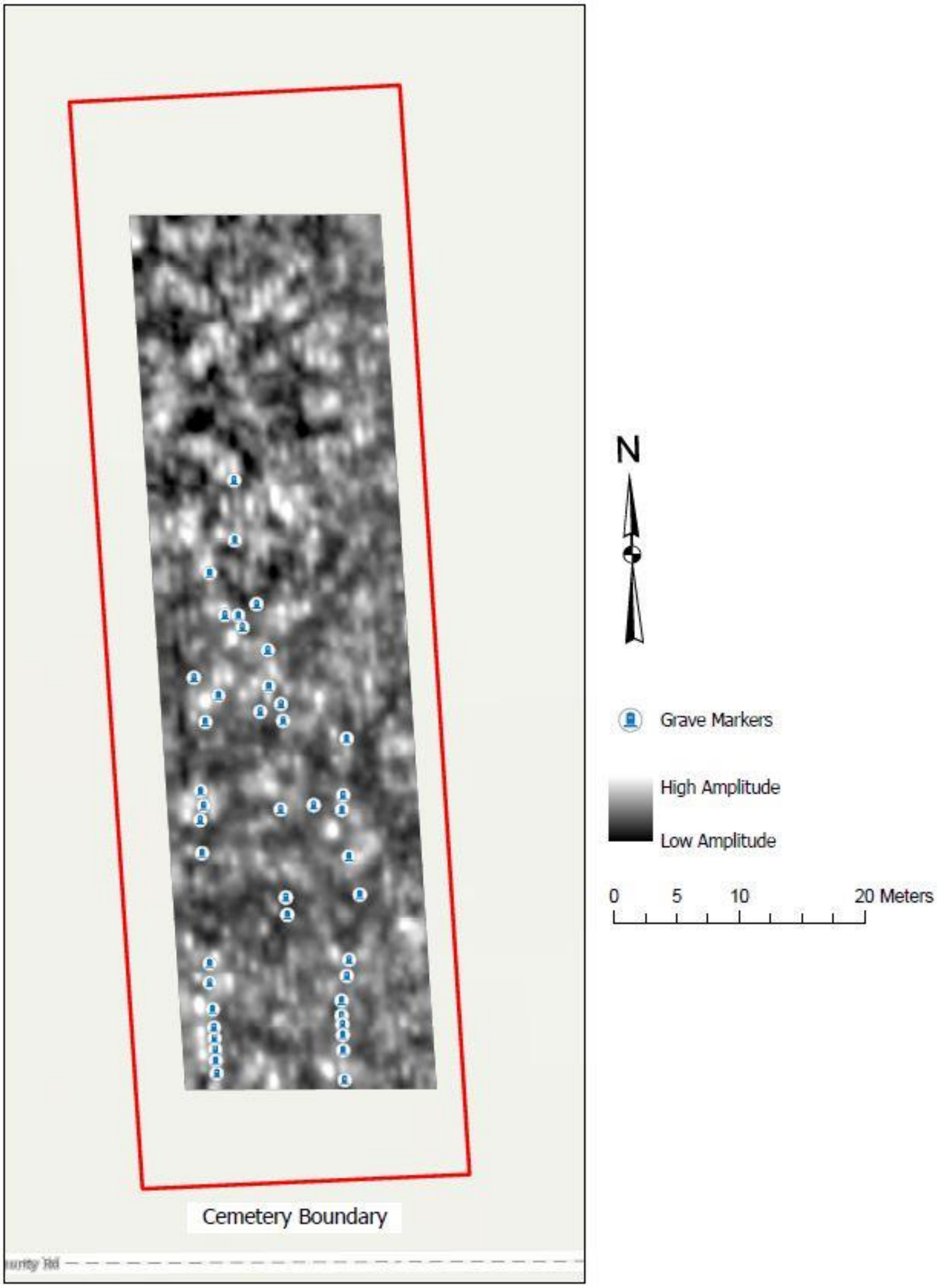

Figure 31: Uninterpreted GPR results from Evangelical Lutheran Cemetery.

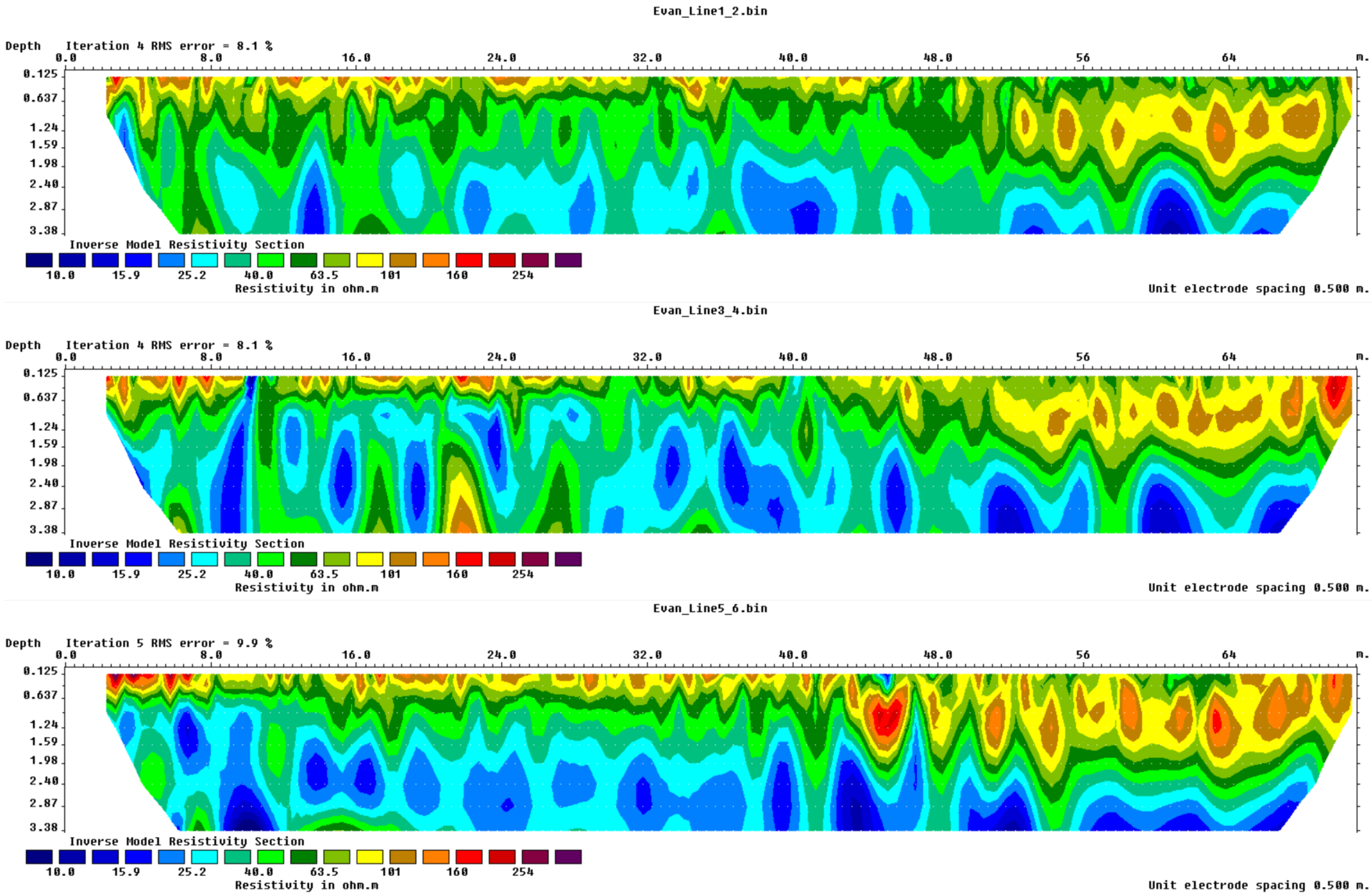

Figure 32: Uninterpreted ERT results from Evangelical Lutheran Cemetery. (Lines 1_2 – 5_6)

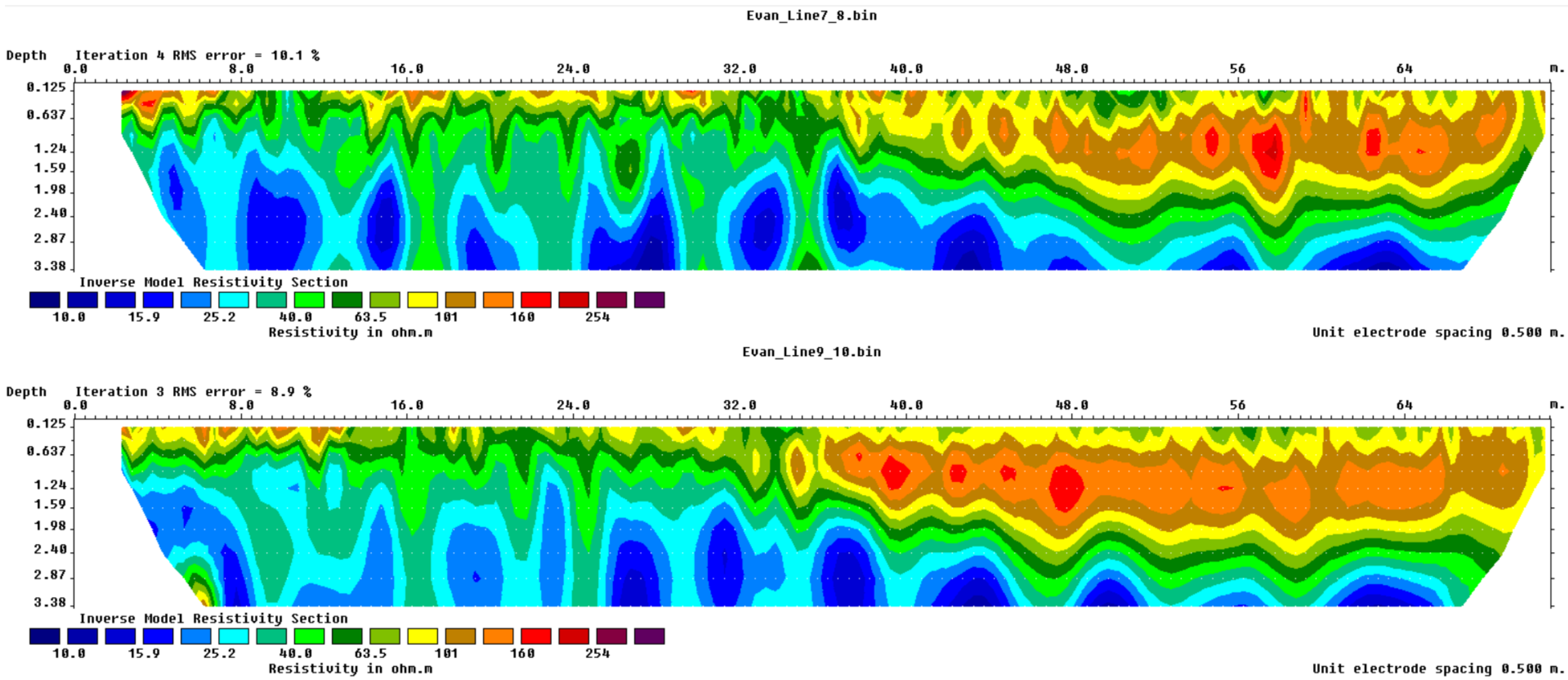

Figure 33: Uninterpreted ERT results from Evangelical Lutheran Cemetery. (Lines 7_8 – 9_10)

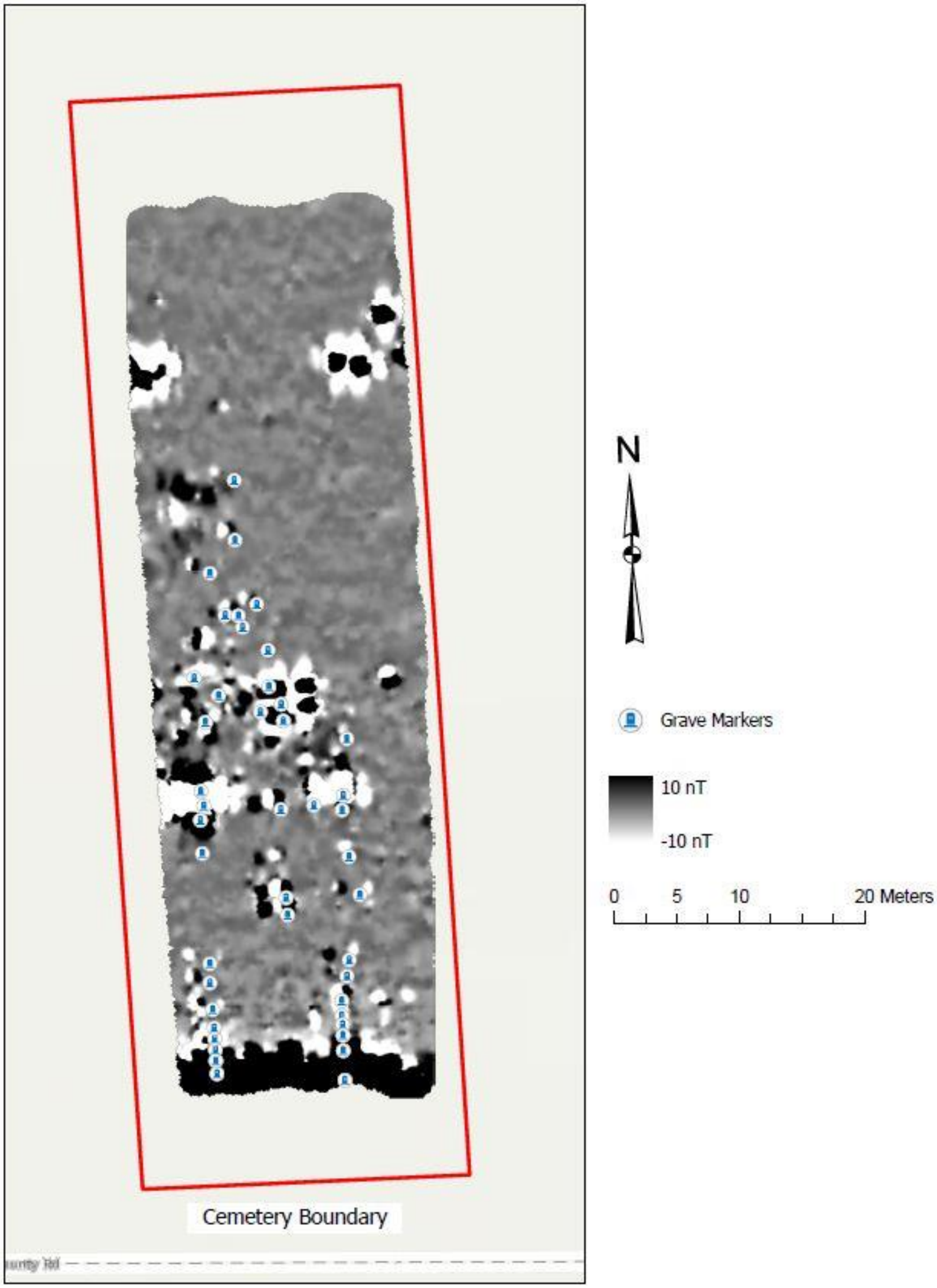

Figure 34: Uninterpreted magnetometry results from Evangelical Lutheran Cemetery.

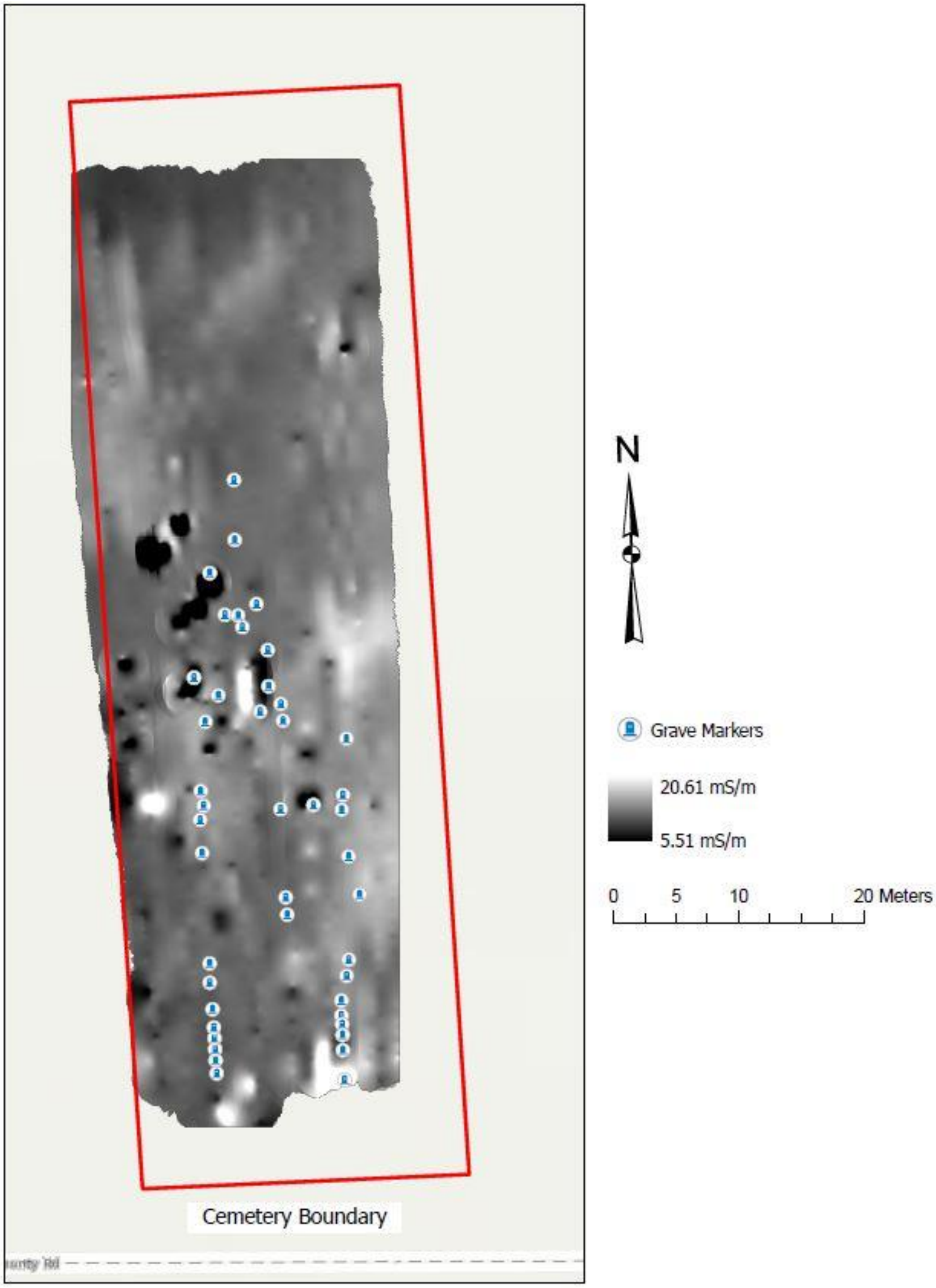

Figure 35: Uninterpreted conductivity results from Evangelical Lutheran Cemetery.

Kingston Cemetery

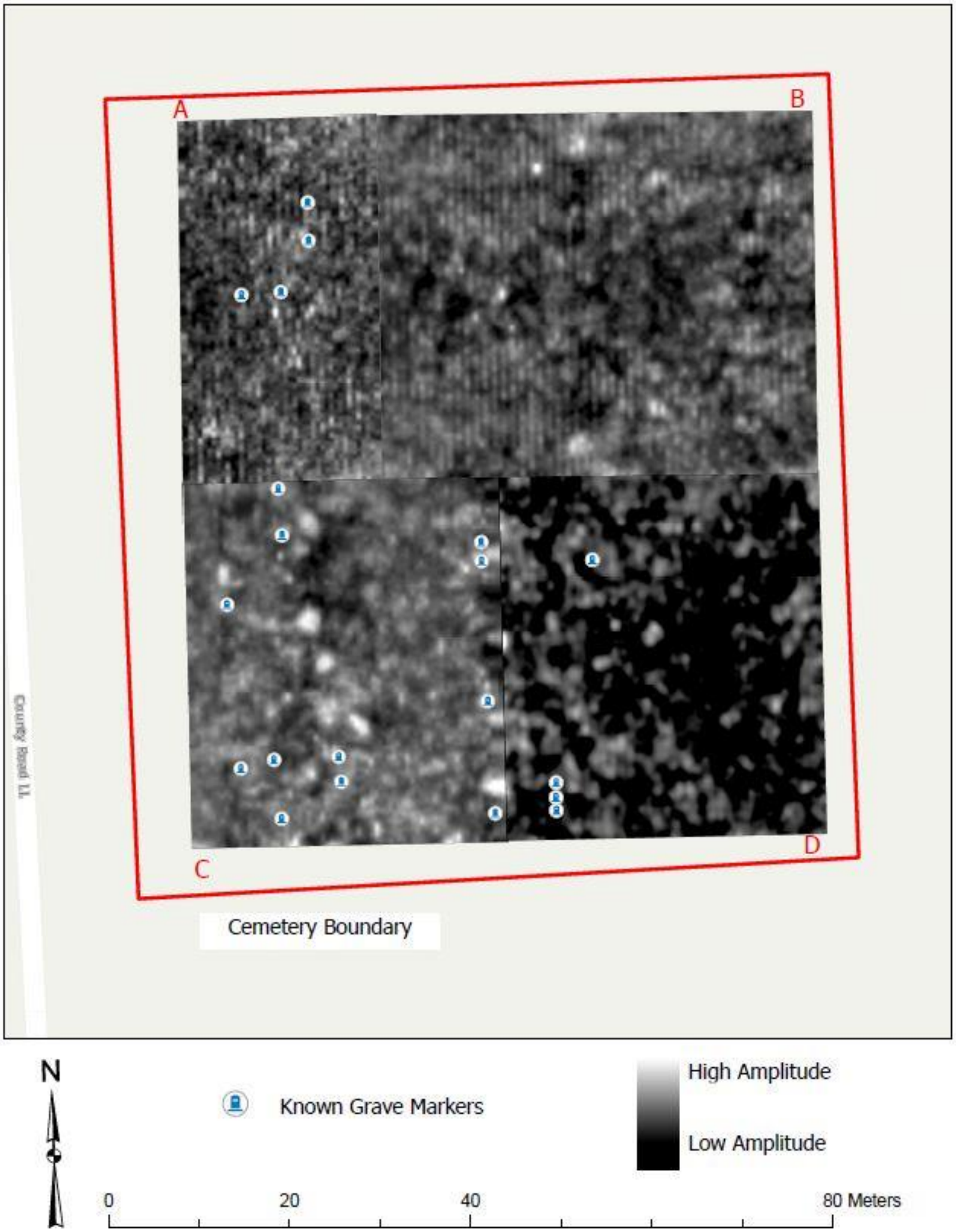

Figure 36: Uninterpreted GPR results from Kingston Cemetery.

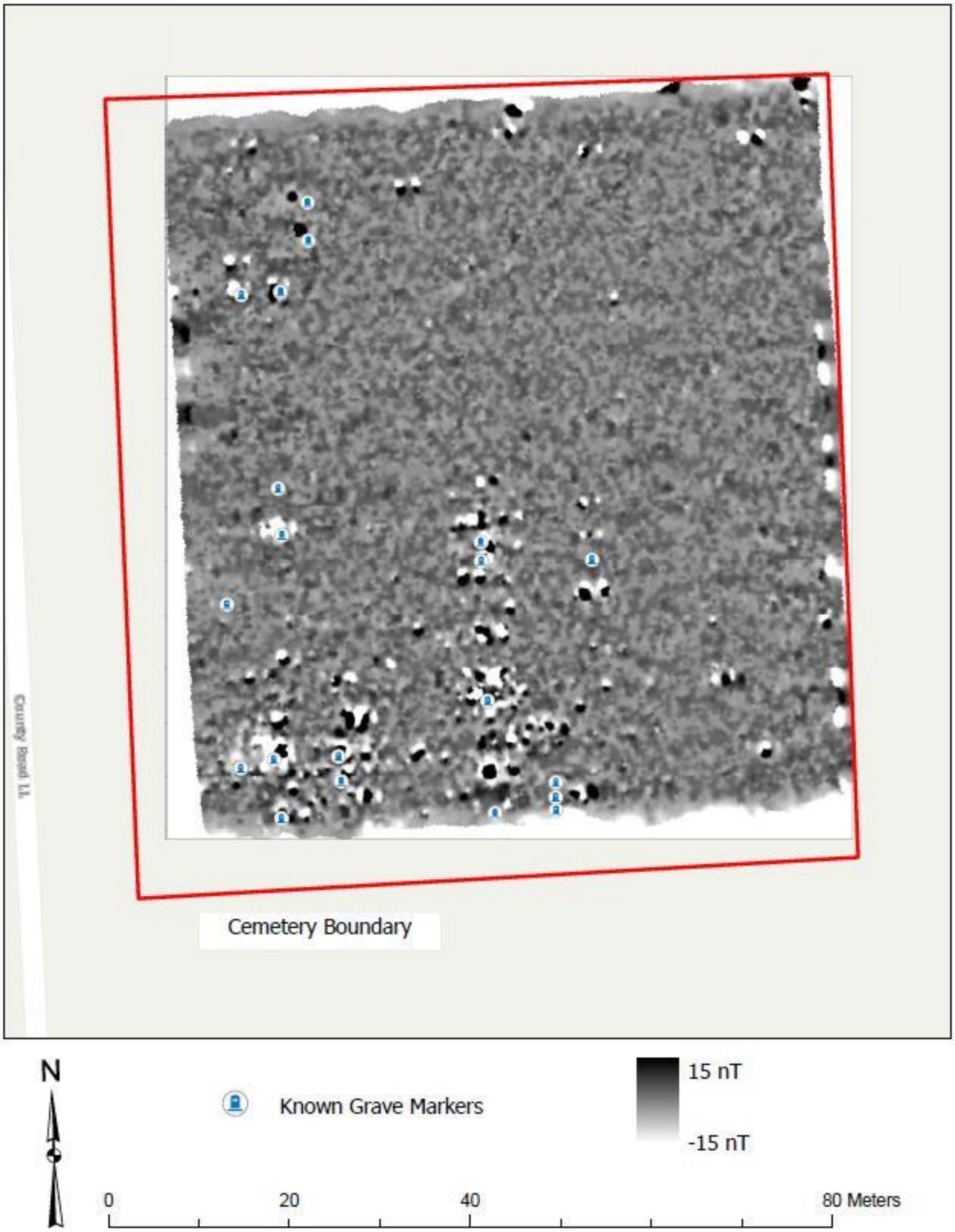

Figure 37: Uninterpreted magnetometry results from Kingston Cemetery.

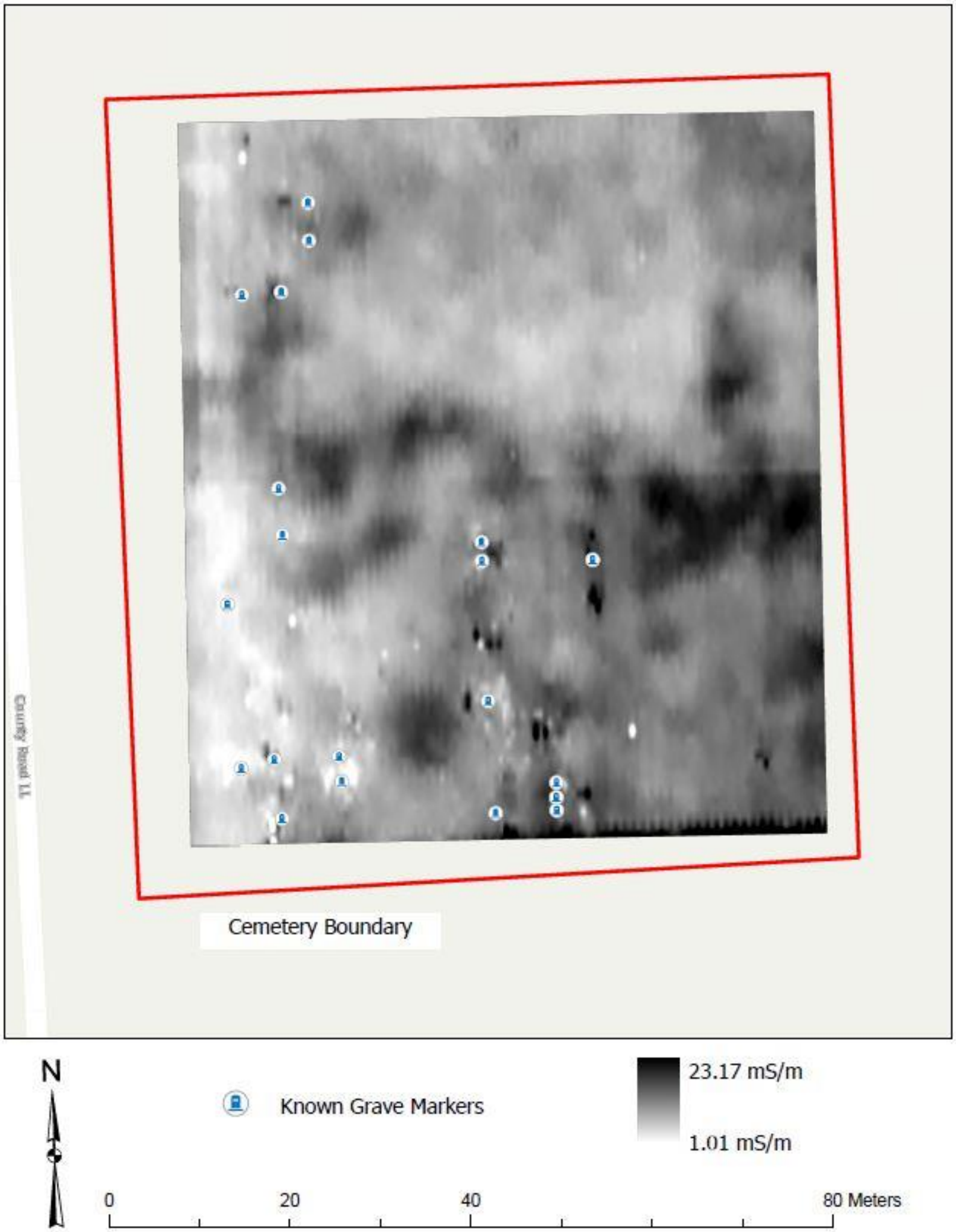

Figure 38: Uninterpreted conductivity results from Kingston Cemetery.